20 Biologically Based Lung Dosimetry and Exposure–Dose–Response Models for Poorly Soluble Inhaled Particles*

Lang Tran
Institute of Occupational Medicine

Eileen Kuempel
Risk Evaluation Branch,
CDC National Institute for Occupational Safety and Health

CONTENTS

* Disclaimer: The findings and conclusions in this chapter are those of the authors and do not necessarily represent the view of the National Institute for Occupational Safety and Health.

20.1 INTRODUCTION

Inhaled airborne particles may be deposited in the respiratory tract with a probability that depends on the physical properties of the particles, the velocity of the air, and the structure of the airways. Once deposited, particles may be retained at the site of deposition, translocated elsewhere in the body, or cleared by the biological processes specific to each region of the respiratory tract.

The major regions of the human respiratory tract include the extrathoracic (nasopharynx or head airways), thoracic (tracheobronchial airways), and alveolar (pulmonary or gas-exchange) (ICRP 1994). These regions differ in structure and function (Miller 1999; McClellan 2000). The functions of the extrathoracic and thoracic regions include air conditioning and conducting, while the main function of the alveolar region is the gas exchange. Clearance of particles depositing in the alveolar region occurs primarily by alveolar macrophage (AV)-mediated clearance to the thoracic region, where they are cleared via the "mucociliary escalator" and then expectorated or swallowed. All regions of the respiratory tract include lymphatic tissue. The extrathoracic region drains to the extrathoracic lymph nodes, and the thoracic and alveolar regions drain to the thoracic (also called hilar) lymph nodes. Particles that are not cleared from the lungs may enter the lung interstitium and translocate to the lymph or blood circulation.

Several terms have been adopted to describe particles based on their size and probability of deposition within the respiratory tract. Inhalable particles are those capable of depositing anywhere in the respiratory tract. Thoracic particles are those capable of depositing in the lung airways. Respirable particles are those capable of depositing in the gas exchange region of the lungs (ACGIH 2005). The respirable particle size distribution includes the ultrafine or nanoparticles (primary particle diameter <0.1 μm), fine particles (<2.5 μm), and coarse particles with diameters <10 μm.

20.1.1 Comparison of Human and Rodent Lung Structure and Physiology

Humans and rodents have in common the major respiratory tract regions, but differ in the structural and physiological details of each region. For example, rats are obligate nose breathers, while humans breathe through either the mouth or nose, depending on the level of exertion and other factors. The nasal airways in rats are more extensive, and the particle deposition fractions in this region are greater than in humans. Conversely, particle deposition fractions in the tracheobronchial region are greater in humans than in rats. Deposition occurs primarily by particle-airway impaction in that region. Rats have an asymmetric (monopodial) branching system of tracheobronchial airways, while primates including humans have a symmetric (bipodial or tripodial) branching system (Crapo et al. 1990). Humans have respiratory bronchioles leading to the alveolar ducts while rats do not, instead having terminal bronchioles leading directly to the alveolar ducts. Yet, the alveolus structure, where gas exchange occurs, is similar in rodents, humans, and other mammals (Mauderly 1996). Because of the structural and size differences in the human and rat respiratory tract, the particle sizes that are inhalable differ in rats and humans (Ménache, Miller, and Raabe 1995).

Humans also differ from rats in physiological factors such as breathing and metabolic rates. Normal alveolar clearance is approximately 10 times faster in rats than in humans (Snipes 1989). Tracheobronchial clearance is relatively rapid in both rats and humans (retention half-times from hours to days), although in humans it has been shown that some particles that deposit in the airways are cleared more slowly (Stahlhofen, Scheuch, and Bailey 1995). The fraction of slowly cleared particles from the lung airways has been shown to increase with decreasing particle size from 6 to <1 μm geometric diameter (Kreyling and Scheuch 2000). This may be an important retention mechanism for nanoparticles, as well. The particle concentration in the lung airways (and particularly at airway bifurcations and centriacinar region) has been associated with both cancer and non-cancer lung diseases (Churg and Stevens 1988; Churg et al. 2003).

Particles that deposit in the alveolar region are associated with the slowest clearance phase in both rats and humans, with normal retention half-times of approximately 2 months in rats and from months to years in humans (Bailey, Fry, and James 1985). The rate of alveolar clearance can depend on the particle exposure concentration and duration in both rats and humans. For example, in coal miners, little or no clearance of particles was observed to occur after retirement from mining (Freedman and Robinson 1988; Kuempel et al. 1997). In rats (and mice and hamsters) with sufficiently high exposures, "overloading" of lung clearance has been observed at greater lung burdens and longer retention times than expected based on studies at lower exposures (Morrow 1988; Muhle et al. 1990; Elder et al. 2005).

20.1.2 Lung Dosimetry Models

The differences in human and rat lung structure and physiology that influence the kinetics of particle deposition and clearance can be described using biologically based mathematical models. Also called lung dosimetry models, these models describe the relationship between the external exposure to airborne particles and the internal dose of particles in the lungs. Biomathematical models that describe the exposure–dose relationship of a toxicant over time are called toxicokinetic models, while those describing the dose–response relationship are called toxicodynamic models. Although less common, models that describe the exposure, dose, and response relationships are called toxicokinetic/toxicodynamic models.

Lung dosimetry models have been developed for several species, but mostly in rats and humans. These models often focus separately on the processes of particle deposition or clearance/retention, although some have been integrated in software programs for humans (ICRP 1994; NCRP 1997; CIIT and RIVM 2002) and rats (CIIT and RIVM 2002). In several earlier rat models, the lungs have been described as a single compartment, with a dose-dependent clearance rate coefficient to account for overload (Yu et al. 1988; Yu and Rappaport 1997; CIIT and RIVM 2002). Other rat models described the lung clearance of insoluble particles during chronic exposure in terms of clearance to the tracheobronchial region, transfer to lymph nodes, and sequestration within the alveolar region (Vincent et al. 1987; Jones et al. 1988; Strom, Johnson, and Chan 1989; Stöber, Morrow, and Hoover 1989; Stöber, Morrow, and Morawietz 1990a; Stöber et al. 1990b). Of the human lung dosimetry models, many have focused on particle deposition. The human multiple path particle deposition (MPPD) model (CIIT and RIVM 2002 includes options for lung morphology based on data by Yeh and Schum (1980), Mortensen et al. (1988), or Koblinger and Hofmann (1990). Other deposition models include an empirical (data-based) model of ultrafine aerosol deposition in the human tracheobronchial airways (Zhang and Martonen 1997) and a stochastic model of particle deposition, with parameters described as statistical distributions based on experimental measurement, which allows for intra- and inter-individual variation in deposition due to lung structure and geometry (Koblinger and Hofmann 1985). Human lung dosimetry models have recently been reviewed by Martonen, Rosati, and Isaacs (2005).

In this chapter, two biomathematical models of the long-term clearance and retention of inhaled particles in rats or humans are described in detail. These include a biologically based model of

exposure–dose–response in rats (Tran et al. 1999, 2000) and a human exposure–dose model calibrated and validated using data from two independent cohorts of coal miners in the U.S. (Kuempel 2000; Kuempel et al. 2001a, 2001b) and the U.K. (Tran and Buchanan 2000). The features of each of these models are unique compared with other existing models. The rat model is the only toxicokinetic/toxicodynamic model currently available for poorly soluble particles. The human model structure is biologically based and is the only clearance/retention model to be validated using human particle lung burden data. The structures of these human and rat models are compatible, which facilitates biologically based extrapolation from the rat to the human for those parameters that are not available for humans. Finally, examples are provided of using these models in risk assessment of occupational exposure to poorly soluble particles.

20.2 MATHEMATICAL MODEL OF THE RETENTION AND CLEARANCE OF PARTICLES FROM THE RAT LUNGS

Mathematically, the deposition and clearance process is a dynamic system, which can be described as a series of compartments. For example, in this model, X_i represents the quantity of free particles on the alveolar surface. Generally, the change in the particle burden in compartment i, dX_i/dt, is described by equations of the form

$$\frac{dX_i}{dt} = D + I_{ij} - O_{ik} \tag{20.1}$$

where

$D =$ input from outside the system to compartment i,
$I_{ji} =$ input from compartment j to compartment i,
$O_{ik} =$ output from compartment i to compartment k.

Equation 20.1 is called the "mass balance" Equation (because, over a set of compartments, mass is preserved).

If the rate of transfer of particles from compartment j to compartment i is assumed to be directly proportional to the mass of particles resident in compartment j, i.e.,

$$I_{ij} = k_{ij}X_j \tag{20.2}$$

then Equation 20.2 is called the "mass action" type and k_{ij} the "transfer rate" is the fraction per unit time.

For multiple inputs and outputs Equation 20.1 can be generalized as

$$\frac{dX_i}{dt} = D + \sum_{j=1}^{m} I_{ji} - \sum_{k=1}^{n} O_{ik} \quad i = 1, \ldots, l \tag{20.3}$$

where m is the number of compartments that output to compartment i, n is the number of compartments that receive output from compartment i and l is the total number of compartments which make up the system.

A system of equations such as Equation 20.3 can represent the dynamics of the retention and clearance of particles/fibres in the alveolar region of the lung.

20.2.1 Structure of the Rat Biomathematical Lung Model

The model is defined by a set of differential equations, which describe the rates at which the quantities of particles in the various compartments are assumed to change. Below we describe

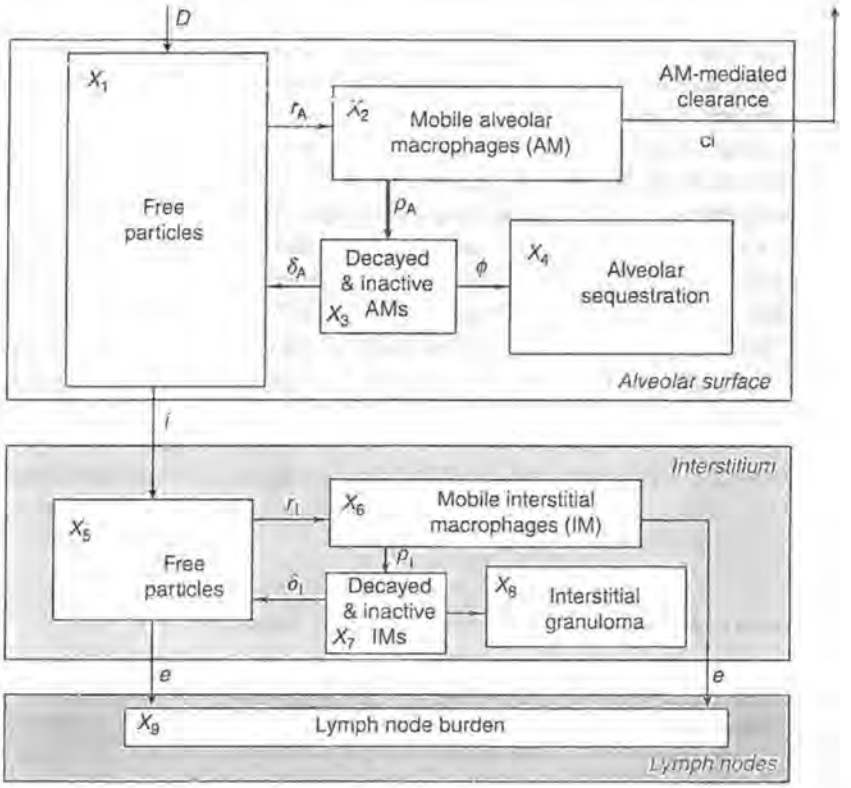

FIGURE 20.1 Schema of the compartments (X_1–X_9) and the transfer rates between compartments.

these compartments, the scientific assumptions about the translocations between them, and the rate parameters governing these processes.

20.2.1.1 Compartments of the Model

Our mathematical model describes the progress over time of the retention of particles and the alveolar macrophage (AM)-mediated clearance process in the pulmonary region, together with the particle redistribution and the overload phenomena. Figure 20.1 shows the nine conceptual compartments describing the location of inhaled particles, plus the main translocation routes between them, including AM-mediated clearance (Tran et al. 1999, 2000).

In Figure 20.1, inhaled particles in the respirable size range can reach the alveolar region of the lung, where they come into contact with epithelial cells. The mass (mg) of free particles on the alveolar surface is represented by compartment X_1. As the result of this contact, these particles are readily transferred into the interstitium (compartment X_5 represents the amount of free particles in the interstitium). This process is likely to be dependent on particle size (Ferin, Oberdörster, and Penney 1992; Oberdörster, Ferin, and Lehnert 1994; Geiser et al. 2005). However, the particle-epithelial cell contact also generates chemotactic signals that attract AMs to the site of particle deposition (Warheit et al. 1988; Reynolds 2005). The ensuing phagocytosis by AMs endeavors to clear the alveolar surface of particles (and thus prevent interstitialisation). Subsequently, the ingested particles are removed by migrating AMs to the mucociliary escalator. (Compartment X_2 represents the amount of particles inside mobile, active AMs.) However, these cells have a finite lifespan. AMs eventually decay and become inactive (compartment X_5 represents the amount of particles inside decayed AMs) and release

their particle load onto the alveolar surface for re-phagocytosis by other, more effective, AMs. Free particles that cross the alveolar epithelium into the interstitium may encounter interstitial macrophages (IMs) and the same events, as described above, are repeated (compartment X_6 represents the amount of particles inside mobile IMs and X_7 represents the particle amount inside decayed IMs). However, from the interstitium, some particles (both free and inside IMs) are removed to the lymph nodes (represented by compartment X_9).

As the particle-epithelial cells contact progresses, AMs become increasingly retained in the alveolar region where they phagocytose *until* they become overloaded. As overloaded AMs decay, this load becomes increasingly difficult to redistribute to more effective AMs (i.e., the macrophages that ingest this particle load will, in turn, become overloaded). Gradually, a "sequestration" pool of particles emerges, consisting of particles in overloaded AMs. This is represented by compartment X_4. Similarly, interstitial granulomas are assumed to be derived from overloaded IMs. The amount of particles sequestered in granulomas is represented by compartment X_8 in the model. Table 20.1 gives a summary description of each of the compartments. The retention of particle-laden AMs occurs together with the recruitment of polymorphonuclear leukocyte (PMN) cells into the affected region—this is the hallmark of the inflammatory process (Donaldson and Tran 2002).

20.2.2 Mathematical Formulation of the Rat Lung Model

20.2.2.1 The Mathematical Description of the Normal (Non-Overload) Retention and Clearance of Particles

20.2.2.1.1 On the Alveolar Surface

The rate of change of the mass of free particles (in mg day^{-1}) consists *primarily* of the deposition of particles from the aerosol, the phagocytosis by AMs, and the interstitialisation of these particles, and *secondarily*, of the release of particles from macrophages which reach the end of their lifecycle

TABLE 20.1
The Compartments in the Model Representing the Location of Particles and the Level of Inflammation

Symbol	Location of Particles
	On the alveolar surface
X_1	Free on alveolar surface
X_2	Successfully phagocytosed by alveolar macrophages
X_3	In inactive alveolar macrophages, can be released for re-phagocytosis
X_4	Sequestered in overloaded, immobile alveolar macrophages
	In the interstitium
X_5	Free in interstitium
X_6	Successfully phagocytosed by interstitial macrophages
X_7	Attached to inactive interstitial macrophages, can be re-released for phagocytosis
X_8	Interstitial granuloma
	At the lymph nodes
X_9	Thoracic lymph nodes
	PMN recruitment
PMN	Number of PMN cells in the alveolar region

$$\frac{dX_1}{dt} = D - r_A X_1 - iX_1 + \delta_A X_3 \tag{20.4a}$$

where

X_1 is the mass (mg) of free particles remaining on the alveolar surface;
D is the dose rate of particles deposited on the alveolar surface (mg day^{-1}), calculated from Equation 2.4b;
r_A is the rate of phagocytosis by AMs (day^{-1});
i is the rate of interstitialisation (day^{-1});
X_3 is the mass (mg) of particles in macrophages in the inactive phase of their lifecycle; and
δ_A is the death rate for inactive macrophages.

The deposited dose rate D of deposited particles (in mg day^{-1}) is calculated as

$$D = \text{Concentration} \times \text{Ventilation rate} \times \text{Daily Exposure period} \times \text{Alveolar deposition fraction} \times (5/7) \times (6/100) \tag{20.4b}$$

where

Concentration is the aerosol concentration (mg m^{-3});
Ventilation rate is the breathing ventilation rate of the rat (l minute^{-1});
Daily Exposure period is the duration of each daily exposure (hr day^{-1});
Alveolar deposition fraction is the fraction of the inhaled particles of a given size deposited in the alveolar region;
(5/7) converts the concentration for a five-days-per-week inhalation pattern into the equivalent average concentration for the 7-days week; and
(6/100) converts the units of the breathing rate to match the time and volume units of the concentration and exposure period.

The alveolar deposition fraction, used in Equation 20.4b, was derived in two ways: (i) from the assumption that inhaled particles are of the (Mass Median Aerodynamic Diameter) MMAD size, and also (ii) from the measured particle size distribution, and using experimental data on the alveolar deposition efficiency for particle inhaled (Raabe et al. 1988).

The transfer rate coefficients (D, r_A, i, etc.) in these equations are shown in Figure 20.1 next to their translocation routes. The coefficients i, δ_A are approximately constant when the lung burden is low, but at higher lung burden the macrophage mediated clearance becomes impaired and the transfer rates become functions of the alveolar particle surface area, s_{alv}, and the form of this dependence is described later. This assumes that the dependence is on the sum of particles which are available to the AMs, i.e., dependence on $s_{alv} = s(X_1 + X_2 + X_3 + X_4)$, where s is particle-specific surface area (in unit of area *per* unit of mass). The phagocytosis rate is left constant for the range of particles to be modeled presently. However, it is envisaged that phagocytosis will become less effective as AMs are expected to clear larger epithelial areas, (covered by particles with larger surface areas). This is likely to be true for nanoparticles. However, data is currently lacking for a reasonably accurate model.

Equation 20.4a, with these coefficients written as functions of s_{alv}, becomes

$$\frac{dX_1}{dt} = D - r_A X_1 - i(s_{alv})X_1 + \delta_A(s_{alv})X_3 \tag{20.4c}$$

Particles that have been phagocytosed by macrophages will subsequently either be removed from the alveolar region by way of macrophage migration and the mucociliary escalator or be released onto the alveolar surface upon the necrosis of AMs. So the rate of change of the mass of phagocytosed particles in active AMs (i.e., X_2) is

$$\frac{dX_2}{dt} = r_A X_1 - \mathrm{cl}(S_{alv})X_2 - \rho_A X_2 \tag{20.5}$$

where cl is the AM-mediated clearance rate (day^{-1}), r_A is the phagocytosis rate (day^{-1}), and ρ_A is the transfer rate (day^{-1}) from active AMs to inactive AMs. When this clearance is unaffected by overload, cl is estimated to be 0.015 day^{-1} (Stöber, Morrow, and Hoover 1989). When clearance is affected by overload, then the dependence of cl on s_{alv} is described by Equation 20.13. The phagocytosis rate r_A is assumed to be independent of the particle surface area as AMs are assumed to be locally mobile in the alveolar region and able to phagocytose particles. Also, ρ_A is assumed to be unaffected by the particle surface area.

The mass of particles inside inactive AMs, X_3, is described by

$$\frac{dX_3}{dt} = \rho_A X_2 - \delta_A(s_{alv})X_3 - \phi(s_{alv})X_3 \tag{20.6}$$

where δ_A is the release rate of particles from inactive AMs back to the alveolar surface and ϕ is the rate of transfer into the alveolar sequestration compartment. Note that for a certain choice of δ_A and ϕ, $\delta_A + \phi = \text{constant}$.

Equations 20.4 through Equation 20.6 describe the dynamics of translocation of particles on the alveolar surface when the lung defenses are not overloaded. The fourth compartment on the alveolar surface, X_4, becomes involved once the lung becomes overloaded with particles. The rate of change of the amount of particles in the alveolar sequestration compartment (X_4), representing the mass of particles trapped inside overloaded macrophages, is

$$\frac{dX_4}{dt} = \phi(s_{alv})X_3 \tag{20.7}$$

20.2.2.1.2 In the Interstitium

Once particles are interstitialised, they will be phagocytosed readily by IMs. Interstitialised particles that escape phagocytosis, together with the particles phagocytosed by Ims, may eventually be removed to the lymph nodes. Let X_5 be the mass of free particles that are interstitialised, then

$$\frac{dX_5}{dt} = i(s_{alv})X_1 - e(s_{inst})X_5 - r_I X_5 + \delta_I(s_{inst})X_7 \tag{20.8}$$

where

e is the removal rate (day^{-1}) of particles to the lymph nodes;
r_I and δ_I, respectively, the rates of phagocytosis by macrophages and release from inactive macrophages, are assumed to have the same value for IMs as for AMs;
and s_{inst} is the interstitial burden in unit of surface area, i.e. $s_{inst} = s(X_5 + X_6 + X_7 + X_8)$.

Equation 20.8 for IMs is comparable to Equation 20.4c for AMs—the first term on the right hand side of Equation 20.8 is the transfer from alveolar surface (instead of deposition in Equation 20.4c), the second and third terms include X_5 instead of X_1, and the last term includes X_7 instead of

X_3. Similarly, the mass of particles phagocytosed by IMs is

$$\frac{dX_6}{dt} = r_1(s_{inst})X_5 - e(S_{inst})X_6 - \rho_1 X_6 \tag{20.9}$$

where the removal rate to lymph nodes (e) is assumed to be the same for IMs as for interstitialised free particles.

The mass of particles trapped in interstitial granulomas is described by

$$\frac{dX_7}{dt} = \rho_1 X_6 - \delta(s_{inst})X_7 - \upsilon(s_{inst})X_7 \tag{20.10}$$

where the transfer rate of particles from active IMs to inactive IMs (ρ_1) and the release rate from inactive IMs (δ_1) are also assumed to have the same dependence on the relevant burden (interstitial or alveolar particle surface area), and also the same non-overload values as for AMs; υ is the rate (day^{-1}) of interstitial granuloma formation which occurs when the IM defense of the interstitium becomes impaired.

The conditions relating to the transfer of particles to interstitial granuloma (X_8) are linked with overload and therefore are described in the section on overload (later). However, the mass of particles trapped in interstitial granulomas is described by

$$\frac{dX_8}{dt} = \upsilon(s_{inst})X_7 \tag{20.11}$$

20.2.2.1.3 At the Lymphatic Level

The mass of particles accumulated in the mediastinal lymph nodes is the sum of the transfer from free interstitialised particles (X_5) and particles in IMs (X_6)

$$\frac{dX_9}{dt} = e(X_5 + X_6) \tag{20.12}$$

20.2.2.2 Mathematical Description of Overload

As described earlier, the impairment of pulmonary clearance during exposure due to overload correlated with the increase in the rate of recruitment of PMNs. The PMN level, in turn, correlated with particle surface area. This impairment of clearance can be described mathematically as a function, θ, of alveolar particle burden (in terms of mass or surface area), which varies between 0 and 1. As θ is a multiplier of the rate parameters, these parameters are fully functioning when $\theta \approx 1$.

Mathematical expressions were developed to describe this progressive impairment. Similar equations were used in other models (e.g., Yu et al. 1988; Stöber, Morrow, and Hoover 1989; Tran, Jones, and Donaldson 1997). Note that all of these functional forms are essentially chosen for practical reasons (i.e., they integrate well with the models in which they form a part). For example, Tran, Jones, and Donaldson 1997 used an exponential decay form

$$\theta(m_{alv}) = e^{-\lambda.(m_{alv}-m_{crit})^{\beta}} \quad \text{for } m_{alv} > m_{crit}$$
$$\theta(m_{alv}) = 1 \quad \text{for } m_{alv} \leq m_{crit}$$

where m_{alv} is the particle mass in the alveolar region and m_{crit} is the critical mass from which impairment begins to manifest. λ and β are parameters controlling the rate and form of decay. This

function has two limitations. First, the parameters of this function cannot be related to some tangible entity, such as mass or surface area. So, it is difficult to judge the plausibility of different values which (λ and β) give a good fit with data. Finally, there is a deterministic boundary at m_{crit} below which there is no impairment—i.e., the equation above provides an abrupt switch over to impairment of clearance. While there is some evidence that this might be the case (Muhle et al. 1990), it is more plausible that impairment would likely progress continuously. Thus, a new functional form for θ in terms of alveolar surface burden, s_{alv}, is introduced

$$\theta(s_{alv}) = 1 - \frac{1}{\left(1 + \left(\frac{s_{1/2}}{s_{alv}}\right)^{\beta}\right)} \tag{20.13}$$

This functional form is similar to that used by Yu and Rappaport (1997) to describe retardation of clearance of insoluble dust. The function is dependent on two parameters, namely $s_{1/2}$ and β. The former, $s_{1/2}$, represents the level of particle surface area such that the impairment is half of its original value; while the latter, β, controls the steepness of the impairment. Figure 20.2 shows the behavior of θ for two different sets of values for β and $s_{1/2}$ over a range of values of s_{alv}. One advantage this function has over the earlier functions from the literature is that one of its parameters, $s_{1/2}$, is readily interpretable and will be useful in the comparison of the effects of different dusts on their retention and clearance.

Since particle surface area affects clearance by mobile macrophages, we assume here that the clearance rate is modified as

$$cl(s_{alv}) = \theta(s_{alv})cl \tag{20.14}$$

where cl, on the right-hand side of Equation 20.14, is the time-independent rate for low lung burdens. Thus, as the particle burden on the alveolar surface (in terms of surface area) increases, mobile macrophages are increasingly retained on the alveolar surface, as described by Equation 20.14. During this phase, particles released by inactive AMs upon death will be less likely to be removed by mobile AMs to the mucociliary escalator (i.e., the transfer rate δ_A, back to the alveolar surface to be re-phagocytosed *and* then cleared by AMs, decreases with increasing alveolar lung burden). Instead, these particles are re-phagocytosed by retained AMs leading to transfer at a rate,

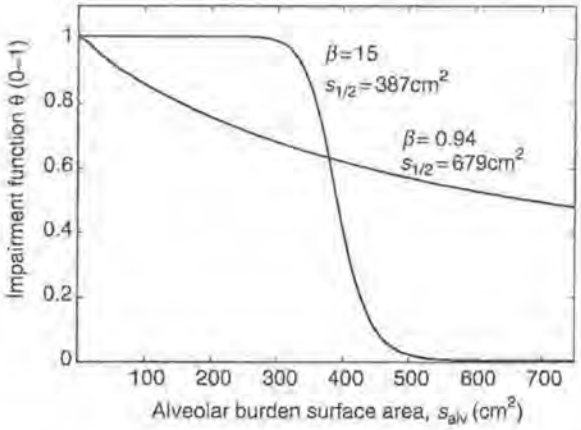

FIGURE 20.2 The impairment function for particle surface area between 0 and 750 cm^2 and two different sets of values for (β, $s_{1/2}$).

ϕ the sequestration rate (day^{-1}), into an alveolar sequestration compartment (X_4). In this case, ϕ increases as impairment develops

$$\phi(s_{alv}) = (1 - \theta(s_{alv}))\phi \tag{20.15}$$

and

$$\delta_A(s_{alv}) = \theta(s_{alv})\delta_A \tag{20.16}$$

For particles with large surface area, as inhalation progresses, there is increasing contact between these particles and epithelial cells, potentially causing damage to these cells. It is assumed that a damaged epithelium will allow greater access of particles into the interstitium (Adamson and Hedgecock 1995). Therefore, the rate of particle interstitialisation increases concurrently with the progression of impairment. Mathematically, the rate of interstitialisation can be modeled as

$$i(s_{alv}) = i_{normal}\theta(s_{alv}) + (1 - \theta(s_{alv}))i_{max} \tag{20.17}$$

where i_{normal} is the rate of interstitialisation under normal conditions and i_{max} is the maximum rate of interstitialisation under complete impairment. So, according to this equation, initially $i(s_{alv}) = i_{normal}$ ($\neq 0$), because AM defense is not absolutely effective and there is always some interstitialisation taking place. Once impairment starts, $i(s_{alv})$ increases from i_{normal} towards i_{max}.

At the interstitial level, we assume that interstitial granuloma will be formed when the defense of the interstitium becomes impaired. There is, however, an absence of data regarding the particulate burden in the interstitium. Therefore, for the present, we are restricted to constructing the framework for this part of the model. This framework is presented to show how the concepts can be included, although the choice of values for the transfer rates will be limited to being plausible (but unsupported) and they will also be chosen so as not to affect the predictions of quantities which can be tested by the existing data (for lymph node burdens).

For the current model, we assume that the impairment of clearance for IMs by dust loading has the same form of dependence on dust loading as for the AMs. We also assume that the impairment of motility follows the same dependence on the impairment function θ, thus

$$\upsilon(s_{inst}) = (1 - \theta(s_{inst}))\upsilon \tag{20.18}$$

The differential equations (Equation 20.4 through Equation 20.18), describing the kinetics of the retention and clearance of particles under normal circumstance (i.e., low exposure and non-impairment of AM defense mechanisms) and for the overload situation, constitute the current mathematical model. The model provides a quantitative, scientifically based representation of the mechanisms of removal of particles from the lung.

The above equations describing the effect of particulate overload describe the process that results in a higher proportion of the lung burden entering the interstitium. The presence of more particles in the interstitium makes more particles available for transfer to the mediastinal lymph nodes. However, there does not appear to be a reason why a higher proportion of the interstitialised particles should be transferred to lymph nodes, so the coefficient for transfer from interstitium to mediastinal lymph nodes (X_9) remains constant.

20.2.2.3 Mathematical Description of PMN Recruitment

In this section, the original model is extended to describe the inflammatory recruitment of PMN cells. There is an association between the mean number of PMNs in the bronchoalveolar lavage

(BAL) fluid and the mean lymph node burden, expressed as surface area (Tran et al. 1999). Since particles found in the lymph nodes were originally interstitialised, the net rate of PMN recruitment is assumed to be proportional to the rate of particle interstitialisation (expressed as particle surface area) and a PMN removal rate that is attributed to normal lifecycle of this type of cell. Thus,

$$\frac{\mathrm{dPMN}}{\mathrm{d}t} = \mathrm{Rec}.\, i(s_{\mathrm{al}}).s.\, X_{\mathrm{I}} - \mathrm{Rem}.\,\mathrm{PMN} \tag{20.19}$$

where PMN represents the number of PMNs ($\times 10^6$) in the BAL fluid. Rec is the number of PMNs recruited *per* unit of dust interstitialised (as surface area). Rem is the removal rate of PMNs (day^{-1}). The specific particle surface area is s and X_{I} is the mass of free particles on the alveolar surface.

20.2.2.4 Summary of Model Parameters

The translocations between the compartments of the model are expressed by *transfer rates* (labeled in Figure 20.1 and defined in Table 20.2). These rates determine the fraction of mass of particles per unit time, which are translocated from one compartment to another (e.g., r, the phagocytosis rate of macrophages, represents the fraction of particles transferred from X_1, the compartment of free particles on the alveolar surface, to X_2 the compartment of successfully phagocytosed particles). In addition to the transfer rates, there are parameters belonging to the impairment function (e.g., β and $s_{1/2}$ in Equation 20.13) and those belonging to the deposited dose D (e.g., breathing rate, deposition fraction, etc.).

TABLE 20.2
The Parameters of the Mathematical Model

Parameters	Symbol	Unit
Deposition		
Deposited dose rate, function of breathing rate, deposition efficiency and exposure concentration	D	$\mathrm{mg\ day}^{-1}$
Kinetics in Macrophages		
Phagocytosis rate by AMs or IMs[a]	r_{A}, r_{I}[a]	day^{-1}
AM-mediated clearance of particles	cl	day^{-1}
Transfer rate of particles from active to inactive AMs or IMs[a]	ρ_{A}, ρ_{I}	day^{-1}
Release rate of particles back to the alveolar surface or interstitium for re-phagocytosis[a]	δ_{A}, δ_{I}	day^{-1}
Kinetics of Particles		
Normal interstitialisation rate of free particles	i_{normal}	day^{-1}
Maximum interstitialisation rate of free particles	i_{max}	day^{-1}
Removal rate of particles to the lymph nodes	e	day^{-1}
Overload and Sequestration		
Alveolar sequestration rate	ϕ	day^{-1}
Rate of formation of interstitial granuloma	υ	day^{-1}
PMN Recruitment		
PMN recruitment rate	Rec	No. of cells recruited *per* unit of particle surface area burden
PMN removal rate	Rem	day^{-1}

[a] The subscripts A and I indicate that the coefficients apply, respectively, to the alveolar and interstitial macrophages.

20.2.3 Model Parameters

20.2.3.1 Parameter Values

Table 20.3 shows the values of the parameters used in the calculation of the deposited dose D (Equation 20.4b). Table 20.4 shows the values of the parameters drawn from previous studies, to be used in the model. The parameters include the phagocytosis rate, which is based on experimental evidence described by Stöber et al. (1989, 1990a, 1990b), indicating that phagocytosis usually takes place within 2–6 h and so, following Stöber, we use the 6 h estimate. This is equivalent to a phagocytosis rate of approximately $1/6 = 0.166\ h^{-1}$, or equivalently $4\ day^{-1}$ when expressed in the same units as the other rates in Table 20.2. The macrophage mediated clearance rate has been estimated as ranging from $0.01\ day^{-1}$ to approximately $0.02\ day^{-1}$, with the value of $0.015\ day^{-1}$ being commonly applicable (e.g., Stöber, Morrow, and Hoover 1989). Estimates of the time scales for the macrophage normal life cycle also based on the evidence presented by Stöber et al. (1990a, 1990b) were used to estimate the rate of transfer from active to inactive macrophages (ρ) and for release from inactive macrophages either for re-phagocytosis (transfer rate δ) or after overload to become trapped in a succession of overloaded macrophages (transfer rate ϕ). For example, if the time scale for the active phase of the life cycle is T_a days, then a population of macrophages in kinetic equilibrium would have a fraction of $1/T_a$ of the active macrophages pass from active to inactive phase each day, so $\rho 1/T_a$. Similarly, there would be a rate of death and release of particles from inactive macrophages δ equal to $1/T_i$, where T_i is the time scale of the inactive phase. Both T_a and T_i have been originally estimated by Stöber et al. (1989, 1990a, 1990b), and values of T_a ($=28$ days) and T_i ($=7$ days) from their studies, corresponding to a reasonable estimate of AM total life cycle of 35 days (van Oud Alblas and van Forth, 1986) were used in our model.

The rate of particulate deposition into the lung was estimated from the volume inhaled, the aerosol concentration, and the alveolar deposition fraction. The values estimated for the breathing rate and alveolar deposition fraction and the plausible range are listed in Table 20.3. A wide range of values for the breathing rate is plausible, as various studies have used markedly different estimates, as shown in the first row of Table 20.3. The alveolar deposition fraction has been measured in rats as a function of the particle aerodynamic diameter by Raabe et al. (1988), giving estimates of 7% for the TiO_2 particles of MMAD ~ 2.1 μm. Table 20.4 shows all the parameters of the model.

TABLE 20.3
Factors Affecting the Deposited Dose

Breathing rate (l/min)	0.1–0.3	Stöber et al. (1994) and Yu et al. (1994)
	0.154	Value used in this study
Target concentrations (mg m^{-3})	50 mg m^{-3}	TiO_2
Exposure regimen	7 h/day	
	5 days/week	
Correction factor (to treat exposure over 5 days as continuous over the week)	5/7 = 0.714	(Also used by Morrow (1988))
TiO_2 deposition fraction	0.07	Original estimates derived from *in vivo* data used in this study, and consistent with values from Raabe et al. (1977) and Raabe et al. (1988)

TABLE 20.4
The *a Priori* Fixed Model Parameter

Parameters	Symbol	Value	Unit
Deposition			
Deposited dose rate, function of breathing rate, deposition efficiency and exposure concentration	D	*see* Table 20.3	mg day^{-1}
Kinetics in Macrophages			
Phagocytosis rate by AMs or IMs[a]	r_A, r_I	4	day^{-1}
AM-mediated clearance of particles	cl	0.015	day^{-1}
Transfer rate of particles from active to inactive AMs or IMs[a]	p_A, p_I	0.036	day^{-1}
Release rate of particles back to the alveolar surface or interstitium for re-phagocytosis[a]	δ_A, δ_I[a]	0.14	day^{-1}
Transfer from overloaded IM to granuloma	ν	0.14	day^{-1}
Kinetics of Particles			
Interstitialisation of free particles, normal rate	i_{normal}	0.03	day^{-1}
Interstitialisation of free particles, maximum rate	i_{max}	1.8	day^{-1}
Removal rate of particles to the lymph nodes	e	0.1	day^{-1}
Overload and Sequestration			
Alveolar sequestration rate	ϕ	0.14	day^{-1}
Rate of formation of interstitial granuloma	ν	0.14	day^{-1}
Impairment Function			
Overload threshold	$s_{1/2}$	387	cm^2
Overload constant	β	15	
PMN Recruitment			
PMN recruitment rate	Rec	0.025	No. of cells *per* unit of s.a. burden
PMN removal rate	Rem	0.01	day^{-1}

[a] The subscripts A and I indicate that the coefficients apply, respectively, to the alveolar and interstitial macrophages.

20.3 EXPERIMENTAL DATA

Two contrasting, poorly soluble "low-toxicity" mineral dusts were used to compare the dose response relationships at exposure concentrations calculated to produce volumetrically similar alveolar deposition rates (Tran et al. 1999). Then, if the dose–response relationships were determined solely by volumetric loading (Morrow 1988), the results would show similarity between the two dusts.

The chosen dusts (Table 20.5) provided contrasting particle sizes with similar densities. Target concentrations (Table 20.6) were calculated from expected alveolar deposition fractions for the size distribution of each dust, accounting for elutriation in the aerosol sampler.

TABLE 20.5
Physical Characteristics of the Test Particles

Dust	Density (g/cm^3)	MMAD (μm)	Specific Surface Area (m^2/g)
Titanium dioxide (TiO_2)	4.25	2.1	6.67
Barium Sulphate ($BaSO_4$)	4.5	4.3	3.13

TABLE 20.6
Target Exposure Concentrations of Respirable TiO_2 and $BaSO_4$

	"Low" Concentration	"High" Concentration
Titanium dioxide (TiO_2)	25 mg m^{-3}	50 mg m^{-3}
Barium Sulphate ($BaSO_4$)	37.5 mg m^{-3}	75 mg m^{-3}
Duration of experiment	203 days	119 days

Rats were sacrificed at 6 time points during exposure for measurement of (i) lung burden, (ii) burden in mediastinal hilar lymph nodes, and (iii) numbers of AMs, lymphocytes, and neutrophils (PMN) in BAL fluid. Groups of 6 rats were used for particulate burdens, and further groups of 6 for BAL.

The lung burdens at the early time points showed that similar mass deposition rates were achieved. However, the $BaSO_4$ lung burdens appeared to latterly approach a steady state level, indicating effective clearance whereas TiO_2 lung burdens continued to increase, (Figure 20.3) consistent with overload, lymph node burdens were higher for TiO_2 (Figure 20.4). Mean numbers of PMNs (inflammation) also increased more rapidly for TiO_2 (Figure 20.5). However,

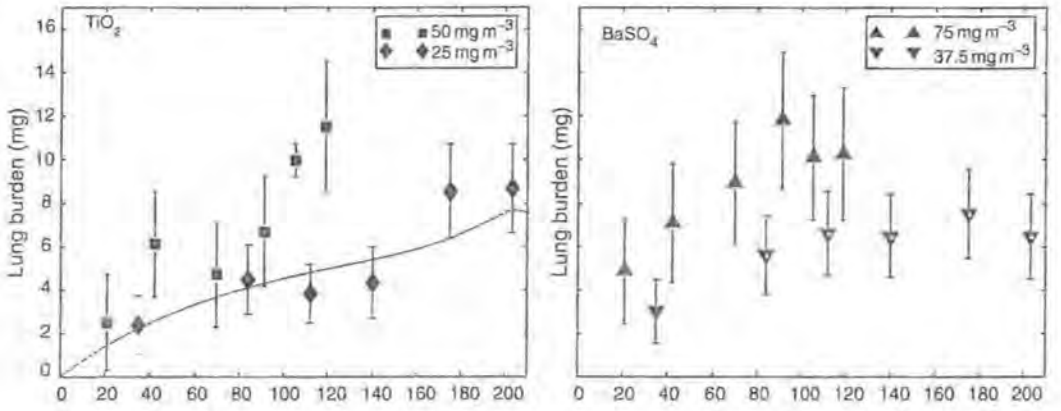

FIGURE 20.3 Mean lung burdens during exposure and model predictions (lines).

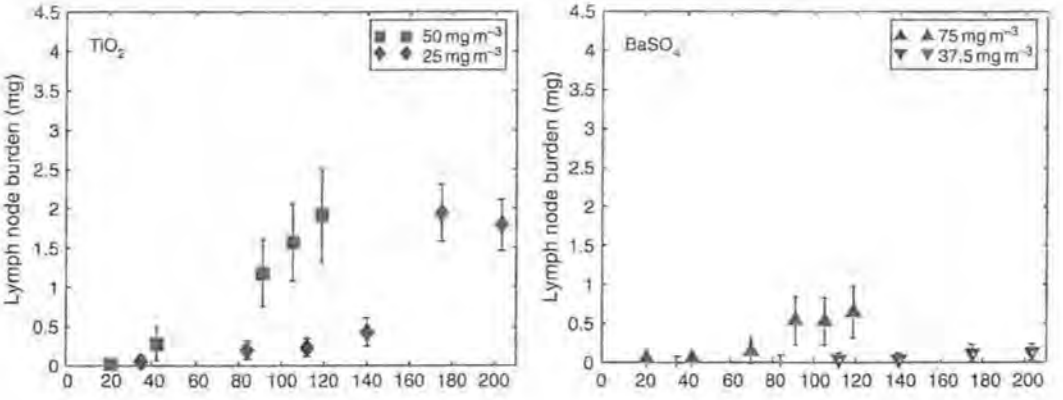

FIGURE 20.4 Mean lymph node burden during exposure and model predictions (lines).

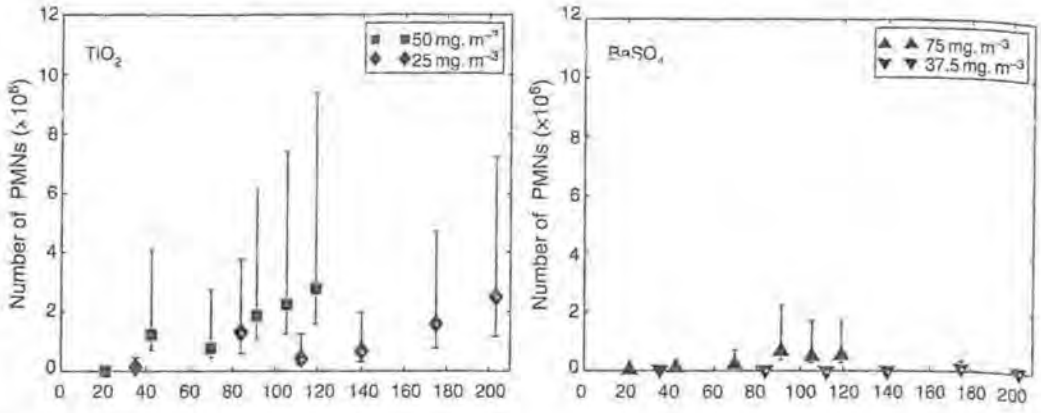

FIGURE 20.5 Mean number of PMN during exposure and model predictions (lines).

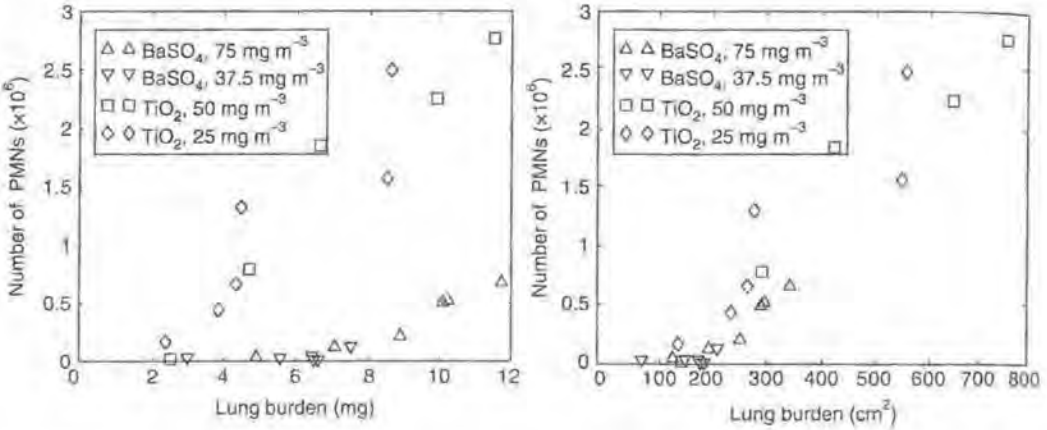

FIGURE 20.6 Mean number of PMN compared to mean lung burdens expressed as mass surface area.

if lung burdens were expressed as surface area, the PMN data for both dusts could be described by a common trend (Figure 20.6).

20.4 STRATEGY FOR MODEL CALIBRATION AND VALIDATION

The lung, lymph node burden, and number of PMNs from the "high" exposure TiO_2 50 mg m^{-3} experiment were used to estimate the non-fixed parameters. Specifically,

1. The lung burden data were used to estimate β and $s_{1/2}$ and the factor for reducing the breathing rate parameter specific to the "high" exposure TiO_2.
2. The lymph node burden *data* were *used* to estimate the translocation rate e.
3. The PMN data to estimate Rec and Rem.

Once these parameters were estimated, the model was fully identified and calibrated. The next step was to validate the model by predicting the outcomes of the "low" exposure TiO_2 experiment and both the $BaSO_4$ experiments and comparing (i.e., checking visually for consistency) with the data from these experiments. (A re-calibration of the model would have been carried out if necessary.)

The model calibration led to the predictions for the "high" exposure TiO_2 shown as the higher lines in Figure 20.3 through Figure 20.5. Model simulations for the "low" exposure TiO_2 experiment and both the $BaSO_4$ experiments (lower lines in Figure 20.3 through Figure 20.5) agreed well visually with the data, thus, we considered the model validated.

20.5 MODEL EXTRAPOLATION TO HUMANS

The four main areas in the exposure–dose–response relationships that are expected to differ between rats and humans are: (i) Exposure Concentration, (ii) Deposited Dose, (iii) Retention and Clearance, and (iv) Cell Recruitment. Occupational human exposure is usually at lower airborne concentration and a longer duration than the exposure in animal studies. The deposited dose is influenced by the ventilation rate and the deposition fraction. Both of these parameters are dependent on the morphology of the lung and are expected to differ between species. Once deposited, particles are either retained or cleared; the retained particles are either interstitialised (parameters i_{normal}, i_{max}) and removed to the lymph nodes (e) or cleared by macrophages (cl). The retention and clearance of particles is known to vary between species (Bailey, Fry, and James 1985). The impairment of particle clearance following overload ($s_{1/2}$) is also known to be species dependent (Bermudez et al. 2002, 2004; Elder et al. 2005).

Table 20.7 lists the model parameters that were either estimated or scaled to humans. The remaining parameters were kept fixed at the values estimated from animal data.

20.5.1 Method for Extrapolation

The following method was used in extrapolating (animal based) model parameters to their human equivalents.

1. For Exposure (Concentration, t_{start}, t_{final})
   We replaced the parameters for concentration and duration with the relevant human occupational equivalents (e.g., 4 mg m^{-3} and working life time of 45 years).
2. For Deposited Dose (Ventilation rate, Deposition fraction)
   We used data available from Hattis et al. (2001) (see Table 20.8).
3. For Retention and Clearance (cl, e, i_{normal}, i_{max})
   We scaled parameters inversely with the ratio of pulmonary surface area to the power 0.25, in accord with the method of Ings (1990). The derivation of this extrapolation factor for kinetic parameters is provided in O'Flaherty (1989).
   e.g., $cl_{human} = cl_{rat}$ (rat pulmonary surface area /human pulmonary surface area)$^{0.25}$. This produces an estimate of the lung clearance rate for humans that is consistent with other estimates of the rate for humans (Bailey, Fry, and James 1985).

TABLE 20.7
Model Parameters to Be Converted to Human Equivalents (For the Definition of the Parameters for Retention, Clearance, and Cell Recruitment, see Table 20.2)

Exposure	Deposited Dose	Retention and Clearance	Cell Recruitment
Concentration	Ventilation rate	cl	Rec
t_{start}	Deposition fraction	e	
t_{final}		$s_{1/2}$	
Daily exposure period		i_{normal}	
		i_{max}	

TABLE 20.8
Central Value for Ventilation Rate, Deposition Fraction and Clearance Rate and Their Distribution

Parameters	Distribution	$\log_{10}$(GSD)	Mean
Ventilation rate	Log-normal	0.12	1.7 (m^3/h)
Deposition fraction[a]	Log-normal	0.30	0.092
Clearance (cl)	Log-normal	0.21	0.0036 (day^{-1})

[a] This depends on the particle MMAD. Abbreviations: MMAD, mass median aerodynamic diameter; GSD, geometric standard deviation.

Source: From Hattis, D., Goble, R., Russ, A., Banati, P., Chu, M., *Risk Anal.*, 21(4), 585–599, 2001.

4. For Threshold Burden ($s_{1/2}$)
   Following Morrow (1988), we expressed the critical lung burden in units of mg/g lung of rat then multiplied by human lung weight to get an absolute value for this parameter for humans. We then converted into particle surface area units using the specific surface area of the TiO_2.
5. For Cell Recruitment (Rec)
   The recruitment of PMN and their removal are events that take place in relation to the particle dose interstitialised from the rat alveolar epithelial surface area. As humans have a much larger surface area, the recruitment rate for PMNs is scaled down with the ratio of pulmonary surface areas (rat/human).
6. For Parameter Distribution
   This approach was applied to all model parameters (Table 20.9) except for the ventilation rate, deposition fraction, and clearance rate, for which we have independent information from Hattis et al. (2001). These parameters' distribution characteristics are given in Table 20.8. One thousand randomly generated parameter sets for humans were generated.

20.5.2 Results

20.5.2.1 Results from Parameter Extrapolation

Table 20.9 shows the mean values for each of the parameters, for rats and for humans. The data available from Hattis et al. (2001) were used to construct the distribution of values for the ventilation rate, deposition fraction, and clearance rate in humans lung surface area is from parent (1992). The results are shown in Figure 20.7.

20.5.2.2 Simulation Results

The human-scaled model was run for the 1000 human parameter sets, for a human population with a 45-year exposure at 4 mg m^{-3} of respirable dust (TiO_2), working on an 8-h shift per day and 250 days per year (Tran et al. 2003). The results for the three main assays: lung burden, lymph node burden, and number of PMN cells, are shown in Figure 20.8.

For each assay, the upper curves represent the 95th, 90th, 85th, and 70th percentiles of the variation. The two lowest curves for each assay are generated using the central values in Table 20.9 and the 5th percentile. At a level of 4 mg m^{-3}, the extrapolated model predicted the occurrence of overload in approximately 30% of the human population. This is indicated

TABLE 20.9
The Rat Based Model Parameters and Their Extrapolated Counterparts

Parameter	Rat	Human
Exposure		
Concentration (mg m^{-3})	4	4
t_{start} (yr)	0	0
t_{end} (yr)	2	45
Deposited Dose		
Deposition fraction	0.06	0.32
Ventilation rate (m^3/h)	0.18	13.5
Hours exposed (h/day)	7	8
Retention and Clearance		
cl (day^{-1})	0.015	0.0036
i_{normal} (day^{-1})	0.03	0.0072
i_{max} (day^{-1})	1.8	0.4347
e (day^{-1})	0.1	0.0242
$m_{1/2}$ (mg)	5.8	4.05×10^{3}
Cell Recruitment		
Rec	0.025	8.67×10^{-5}
Lung Parameters		
Lung weight (gm)	1.43	1000
Lung surface area (cm^2)	4865	1430000

in the retardation of clearance in the build up of lung burden for the 95th, 90th, and 85th percentile curves. The pattern of overload diminished at lower percentiles, and from the 70th percentile, pulmonary clearance of dust is unimpaired. To find the level of airborne concentration such that 95 percent of the population can avoid overload, further extrapolations at lower exposure concentrations were needed. Simulations with stepwise decreases in concentration were made until concentration reached a level such that the 95 percent of the population does not develop overload within a lifetime working exposure. This critical exposure level was found to be 1.3 mg m^{-3}. Also, at this concentration, the predicted PMN level was low compared to the population of AM (7×10^9 cells) (Crapo et al. 1983; Dethloff and Lehnert 1988). Therefore, 1.3 mg m^{-3} could be interpreted as a Non-Observed-Adverse-Effect-Level (NOAEL) for humans (Trans et al. 1999).

Figure 20.8 and Figure 20.9 show the results of the further extrapolations: the upper curve represents the 95th percentile level for each assay. The central curve is obtained from the central values in Table 20.9 and the lower curve represents the fifth percentile.

20.6 HUMAN LUNG DOSIMETRY MODEL

The work above has illustrated an approach to obtain a human lung dosimetry model by extrapolating the animal-based results. Now, we introduce a biologically based human dosimetric lung model, developed to describe the long-term clearance and retention of respirable particles in the lungs of humans. This model has a unique advantage of being validated with human data.

The data used in developing this model included working lifetime exposure histories of lung burden data from an autopsy study in U.S. coal miners (Vallyathan et al. 1996). Several models describing the plausible mechanisms of particle retention and clearance in humans were initially investigated, including: (1) overloading as observed in rat lungs, (2) particle sequestration in the lung interstitium, and (3) a combination of both processes. The fits of these models to the coal miner

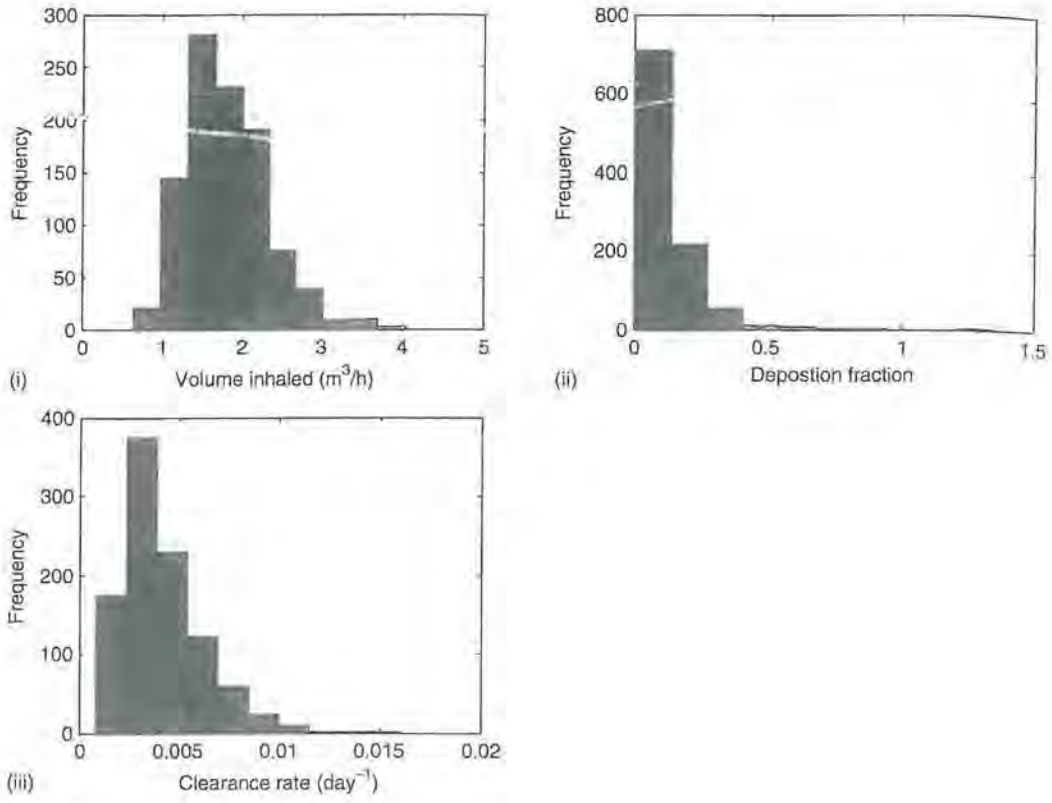

FIGURE 20.7 The distribution for (i) ventilation rate, (ii) deposition fraction, (iii) clearance rate (From Hattis, D., Goble, R., Russ, A., Banati, P., and Chu, M., *Risk Anal.*, 21(4), 585–599, 2001.)

data were evaluated using statistical methods to determine which mechanism may best describe the particle clearance kinetics in the lungs of these humans (Kuempel 2000).

The results showed that a one-compartment rat lung overload model under predicted the lung burdens in the miners with relatively low lifetime exposures and overpredicted the lung burdens in the miners with the higher exposures. This is because at low exposures, the rat model is a simple, first-order kinetic model that predicts effective clearance and very little particle retention in retired miners' lungs. However, at high exposures, the rat model predicts impaired clearance and much higher retained burdens than those actually observed in coal miners.

The model structure that provided the best fit to the coal miner data was a three-compartment, higher-order model with an interstitial or sequestration compartment (Kuempel et al. 2001a). This model includes alveolar, interstitial, and hilar lymph node compartments (Figure 20.10). The form of the model that provides the best fit to the lung dust burden data in these coal miners includes a first-order interstitialisation process and either no dose-dependent decline in alveolar clearance or much less decline than expected from rodent studies.

Key: D is the dose rate of deposited particles; first order rate coefficients include alveolar-macrophage mediated clearance of particles to the tracheobronchial region (K_T), transfer of particles into the pulmonary interstitium (K_I), and translocation of particles to the hilar lymph nodes (K_{LN}); F is an exponential decay function that describes overloading as a dose-dependent decline in K_T; and M is the particle mass in a given lung region, including that cleared to the tracheobronchial region (M_T), or retained in the alveolar (M_A), interstitial (M_I), gas-exchange (M_{LU}), or hilar lymph node (M_{LN}) regions.

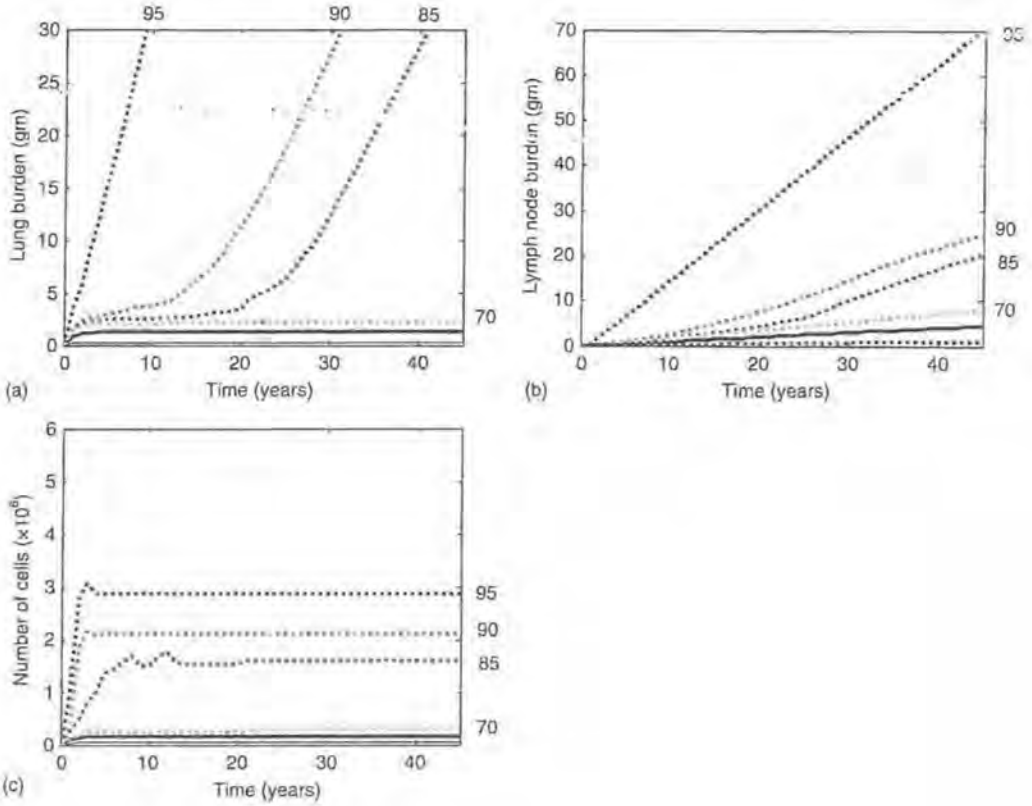

FIGURE 20.8 Simulation of the dose–response to TiO_2 in humans. (a) Lung burden, (b) Lymph node burden, and (c) Number of PMN cells. Each curve represents the 95th, 90th, 85th, and 70th percentile of the variation in each assay. The two lowest curves for each assay are generated using respectively the central value in Table 20.9 and the 5th percentiles.

20.6.1 Model Equations and Description

This three-compartment human lung model describes the kinetics of particle mass transfer in the lungs. The model consists of a series of nonlinear differential equations that are integrated over time to predict individuals' lung and lymph node particle burdens.

The rate of change of particle mass in the alveoli (M_A) at any time (t) is defined as

$$dM_A/dt = R_D - R_T - R_I \tag{20.20}$$

where R_D is the deposition rate (mg/yr) of inhaled, respirable particles into the alveoli (described in Equation 20.21). R_T is the clearance rate (mg/yr) of particles from the alveoli to the tracheobronchi (Equation 20.22). R_I is the transfer rate (mg/yr) of particles from the alveoli into the interstitium (Equation 20.24).

$$R_D = F_D \times C_I \times V_I \times d \tag{20.21}$$

where F_D is the fractional deposition (fraction of the inhaled particle mass that is deposited in the alveolar region of the lungs; C_I is the airborne concentration of dust inhaled (mg/m^3); V_I is the

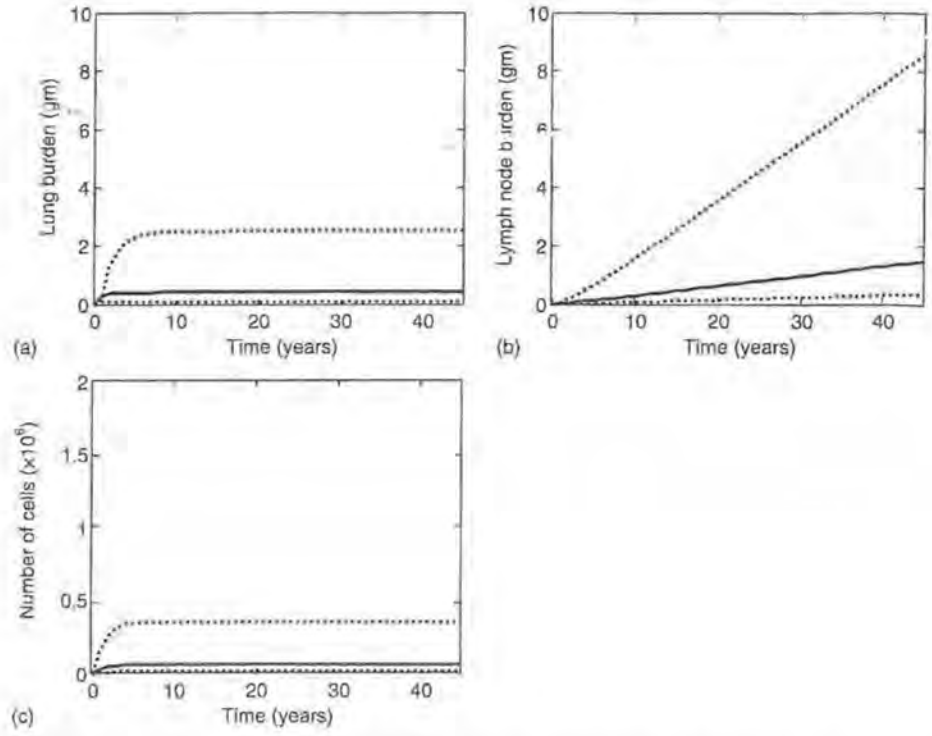

FIGURE 20.9 The dose–response at 1.3 mg m^{-3}. (a) Lung burden, (b) lymph node burden, and (c) number of PMN cells. For each assay, the upper curve represents the 95th percentile of the variation; the two lowest curves are generated using respectively the central values in Table 20.9 and the 5th percentiles.

volume of air inhaled in an 8-h work day (m^3/d); and d is the days worked per year (d/yr) (estimated as 5 days/week × 50 weeks/year).

$$R_T = K_T \times 365 \times F \times M_A \tag{20.22}$$

where K_T is the first-order rate coefficient (d^{-1}) for particle clearance from the alveoli to the tracheobronchi. M_A is defined in Equation 20.20; 365 is the days per year, to convert R_T to units of yr^{-1}; and F is defined in Equation 20.23a and Equation 20.23b.

$$F = 1 \quad \text{when } M_A < M_{min} \tag{20.23a}$$

$$F = \exp\{-B[(M_A - M_{min})/(M_{max} - M_{min})]^C\} \quad \text{when } M_A > M_{min} \tag{20.23b}$$

where F is a dose-dependent modifying factor of K_T. M_{min} and M_{max} are constants representing the human-equivalent minimum and maximum critical lung dust burdens at which the dose-dependent decline in the alveolar clearance rate coefficient begins and reaches a maximum, respectively, as predicted from rodent studies (see next section); M_A is defined in Equation 20.20. When $M_A < M_{min}$, F is set equal to 1; when $M_A > M_{min}$, F equals a value (between 0 and 1) that is determined by B. C is a shape parameter (set to 1 in this model).

$$R_I = K_I \times 365 \times M_A \tag{20.24}$$

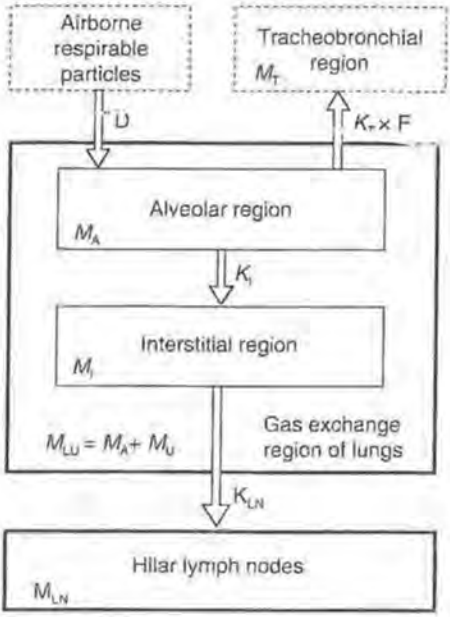

FIGURE 20.10 Three-compartment human lung dosimetry model. (From Kuempel, E. D., O'Flaherty, E. J., Stayner, L. T., Smith, R. J., Green, F. H. Y., and Vallyathan, V., *Reg. Toxicol. Pharmacol.*, 34, 69–87, 2001a. With permission.)

where K_I is the first-order rate coefficient (d^{-1}) for transfer of particles from the interstitium to the lung-associated (hilar) lymph nodes. M_A is defined in Equation 20.20; and 365 converts R_I to units of $year^{-1}$.

The rate of change of particle mass in the interstitium (M_I) at any time (t) is defined as

$$dM_I/dt = R_I - R_{LN} \tag{20.25}$$

where R_I is defined in Equation 20.20 and Equation 20.25. R_{LN} is the translocation rate (mg/yr) of particles from the interstitium to the lung-associated (hilar) lymph nodes, as follows

$$R_{LN} = K_{LN} \times 365 \times M_I \tag{20.26}$$

where K_{LN} is the first-order rate coefficient (d^{-1}) for translocation of particles from the interstitium to the hilar lymph nodes. M_I is defined in Equation 20.25; and 365 converts R_{LN} to units of yr^{-1}.

The rate of change of particle mass in the hilar lymph nodes (M_{LN}) at any time (t) is defined as

$$dM_{LN}/dt = R_{LN} \tag{20.27}$$

where R_{LN} is defined in Equation 20.26.

The mathematical equations in the three-compartment model reflect the biological structures and kinetic processes in human lungs that influence respirable particle clearance and retention. The build-up of particles in the alveolar compartment is determined by the rates of particle deposition, AM-mediated clearance, and particle transfer into the interstitium (Equation 20.20). The deposition of particles in the alveolar compartment is assumed to occur at a rate proportional to the concentration in inhaled air, i.e., a first-order process (Equation 20.21). AM-mediated clearance is

described as a first-order process at lung burdens below those potentially causing impairment of clearance (Equation 20.22). At higher lung dust burdens, AM-mediated clearance can be described as dose-dependent, declining exponentially (Equation 20.23). The model also assumes that some particles will escape phagocytosis by AMs and enter the interstitium at a constant rate (Equation 20.24); this will occur even at low lung dust burdens, below the estimated human-equivalent dose associated with overloading of alveolar clearance. The buildup of particles in the interstitium is described by the difference in the rates of particles entering from the alveoli and particles leaving to the lung-associated lymph nodes (Equation 20.25). The rate of particle translocation to the lymph nodes is also assumed to be first-order (Equation 20.26), and the accumulation of particles in the lymph nodes occurs only by particles passing through the interstitium (Equation 20.27). The rate coefficients for these processes are estimated by the model fitting and parameter estimation (Kuempel et al. 2001a). By suitable integration, the model equations also enable prediction of the amount of dust in the lung and lymph node compartments at any point in time.

20.6.2 Model Parameter Description and Estimation

The initial model parameter values were based on data available in the literature. Some of these parameters were fixed while others were allowed to vary to optimize the model fit to the data. The fixed values include: fractional deposition (F_D) in the alveolar region of the lungs for particles with mass median aerodynamic diameter of 5 μm, assuming mouth breathing at inhalation rate of 1.7 m^3/h (ICRP 1994); the volume of air inhaled (V_I) in an 8-h work day (m^3/d), for heavy work, defined as 7 h of light exercise and 1 h of heavy exercise, for a reference worker (Caucasian, age 30 years, height 176 cm, weight 73 kg) (ICRP 1994); and d is the days worked per year (d/yr) (estimated as 5 days/week×50 weeks/year). The fixed parameters in the expression describing the overloading of alveolar clearance include the estimated human-equivalent lung dust burdens associated with the beginning of decline in the alveolar clearance rate coefficient and the leveling-off of that decline (M_{min} and M_{max}, respectively, in Equation 20.23a and Equation 20.23b above).

The parameter values that were allowed to vary in optimizing the fit of the model to the data were K_T, K_{LN}, K_I, and B. Because a primary objective was to evaluate clearance kinetics of particles in humans, including the possibility of overloading of alveolar clearance as observed in rodents, the deposition parameters were fixed at the average human values in the literature (ICRP 1994), and the clearance parameters were iteratively varied to determine the best fit of the model to the data. A systematic grid search approach was used to determine the parameter values that provided the best fit of the model to the data (Kuempel et al. 2001a). A sensitivity analysis of the model parameter values was performed (Kuempel et al. 2001b). The distribution of clearance rate coefficient was estimated, which provided quantitative information about the plausible particle clearance rates in this cohort (Kuempel et al. 2001b). These values were consistent with values previously reported for long-term particle clearance in humans (Bailey, Fry, and James 1985). The model parameters are described in Table 20.10.

The optimized parameter values and statistical model fit are shown in Table 20.11. The model with the best fit (lowest mean squared error) was the three-compartment model with interstitial-sequestration compartment but with no dose-dependent decline in AM-mediated clearance.

From Table 20.11, the optimal choice, i.e., the three-compartment model with first-order interstitialisation and effective (no overload) alveolar clearance, was chosen and simulated, assuming the mean exposure to respirable coal mine dust among all miners in this study (3 mg/m^3 for 36 years) (Kuempel et al. 2001a). The results are presented graphically in Figure 20.11.

A sensitivity analysis was performed to determine which model parameters are most influential in the model prediction of two key variables: the lung and lymph nodes burden

TABLE 20.10
Description of Variables and Constants in Three-Compartment Human Lung Dosimetry Model

Abbreviation	Units	Description
F_D	None	Fractional deposition of airborne respirable dust in alveolar region
V_I	m^3/day	Volume of air inhaled in 8-h day, heavy work
D	Days/year	Days exposed/year
C_i	mg/m^3	Mean concentration of respirable coal mine dust inhaled, by job[a]
D	Years	Duration of exposure, by job[a]
K_T	day^{-1}	Rate coefficient, alveolar macrophage-mediated clearance to tracheobronchi
K_1	day^{-1}	Rate coefficient, transfer from alveoli to interstitium
K_{LN}	day^{-1}	Rate coefficient, translocation from interstitium to hilar lymph nodes
F	None	Exponential decay function, dose-dependent reduction in K_T
B	None	Slope modifier of F
C	None	Shape modifier of F
M_{min}	mg	Minimum lung dust burden associated with beginning of dose-dependent decline in K_T
M_{max}	mg	Maximum lung dust burden associated with leveling off of dose-dependent decline in K_T

[a] Individual work history data for each miner (input data).

Source: From Kuempel, E. D., O'Flaherty, E. J., Stayner, L. T., Smith, R. J., Green, F. H. Y., and Vallyathan, V., *Reg. Toxicol. Pharmacol.*, 34, 69–87, 2001a. With permission.

(Kuempel et al. 2001b). Each model parameter of the optimal parameter set was allowed to change by ± 10 percent of the central value given in Table 20.11. The summary statistics, mean squared error and mean bias, were calculated for the two variables. The results of this exercise are shown in Table 20.12.

It is clear that any change which results in a higher retention of lung burden, such as a higher deposition, lower clearance, or higher interstitialization, will lead to a higher mean squared error for lung burden. In particular, the predicted lung burden is most sensitive to the deposition rate. For the predicted lymph nodes burden, as expected, the deposition rate and the translocation rate to the lymph nodes are most sensitive.

20.6.3 Application of Human Lung Dosimetry Modeling in Risk Assessment

In this section, we describe an alternative biomathematical modelling approach to that described in Section 20.5. In Section 20.5, a rat-based exposure-dose-response model is extrapolated to humans to predict the working lifetime exposure concentration of TiO_2 that is not likely to result in pulmonary inflammation, based on the rat model. Here, a human-based lung dosimetry model (Sections 20.7.1 and 20.7.2) describing the exposure-dose relationship of respirable particles is used in conjunction with a statistical model of the rat dose-response relationship for particle surface area dose in the lungs and initiation of pulmonary inflammation following inhalation exposure to finesized TiO_2 or $BaSO_4$. This illustrates two different biomathematical modeling approaches to the same rat data (Tran et al. 1999). First, the relationship between particle surface area dose and pulmonary inflammation in rats was investigated using a statistical approach. Statistical models do not explicitly model the biological mechanisms; rather, they involve fitting a mathematical expression to the data. The data used here are from the subchronic inhalation study in rats exposed to fine TiO_2 or $BaSO_4$ (Tran et al. 1999) described earlier. Specifically, individual rat data were obtained for PMN count in the lungs. Different groups of rats were used to estimate retained particle lung burden.

TABLE 20.11
Optimized Parameter Values and Statistical Fit of the Three-Compartment Human Lung Dosimetry Models, by Degree of Overloading of Alveolar Macrophage-Mediated Clearance in Human Interstitial/Sequestration Model

	Model Structure and Optimized Parameter Value		
Model Parameter[a]	No Overload	50% Overload	90% Overload
F_D	0.12	—[b]	—[b]
V_t (m^3/day)	13.5	—[b]	—[b]
d (days/year)	250	—[b]	—[b]
K_T (years)	1×10^{-3}	1.5×10^{-3}	1.4×10^{-3}
K_1 (day^{-1})	4.7×10^{-4}	7.0×10^{-4}	3×10^{-4}
K_{LN} (day^{-1})	1×10^{-5}	1×10^{-5}	1×10^{-5}
B (day^{-1})	0.0001	0.69	2.3
C	1	—[b]	—[b]
M_{min}	1.05×10^{2}	—[b]	—[b]
M_{max}	1.05×10^{5}	—[b]	—[b]
	Statistical Fit of Model to Lung Burden and Lymph Node Burden Data: Mean Squared Error (MSE)		
Dataset	No Overload	50% Overload	90% Overload
All Miners ($n = 131$)	79.3	85.8	231
Miners with hilar lymph node burden data ($n = 57$)	94.7	106	354
	1.31[c]	1.39[c]	2.15[c]
Miners with no post-exposure duration ($n = 11$)	70.0	68.9	148

[a] Parameter description provided in Table 20.10.
[b] Fixed at values in no overload model.
[c] MSE for hilar lymph dust node burden (g).
Source: From Kuempel, E. D., O'Flaherty, E. J., Stayner, L. T., Smith, R. J., Green, F. H. Y., and Vallyathan, V., *Reg. Toxicol. Pharmacol.*, 34, 69–87, 2001a. With permission.

The following piecewise linear model fit was fit to the PMN data (Figure 20.12) (Kuempel et al. 2005, NIOSH 2005).

$$\mu_{PMN}(d_i) = \begin{cases} \beta_0 & d_i < \gamma \\ \beta_0 + \beta_1(d_i - \gamma) & d_i \geq \gamma \end{cases} \tag{20.28}$$

where d_i is the dose for the ith rat; γ is the threshold parameter; B_0 is the mean PMN count for dose of zero or up to γ; and B_1 describes the effect of dose above γ on the mean PMN count.

This nonlinear equation was fit to the data using maximum likelihood estimation of the parameter values. Approximate confidence limits were found using profile likelihood and validated using parametric bootstrap methods. The maximum likelihood estimate (MLE) of the threshold dose was 139 cm^2 (95% confidence interval estimates: 130–144 cm^2), based on the model fit to the TiO_2 and $BaSO_4$ data from Tran et al. (1999). The threshold dose (MLE and CI) was considered the "critical" dose for initiation of pulmonary inflammation in rats, and this critical dose per g of lung tissue was assumed to be the same in rats and humans (i.e., equal sensitivity to equivalent dose assumed) (Jarabek et al. 2005) (Table 20.13). The estimated critical lung dose as particle surface

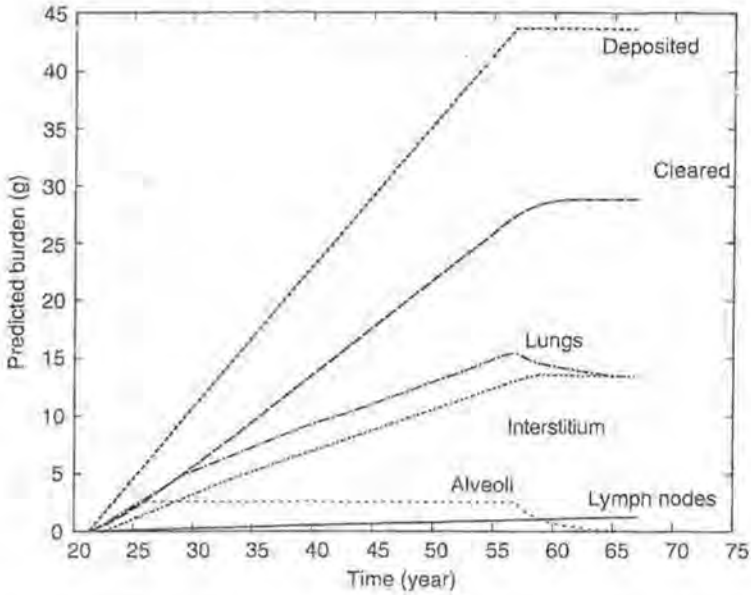

FIGURE 20.11 Predicted mass of particles retained in various lung compartments over time "Deposited" refers to the alveolar region of the lungs, and "cleared" means from the alveoli to the mucociliary clearance path in the tracheobronchial region. (From Kuempel, E. D., O'Flaherty, E. J., Stayner, L. T., Smith, R. J., Green, F. H. Y., and Vallyathan, V., *Reg. Toxicol. Pharmacol.*, 34, 69–87, 2001a. With permission.)

area is the same for fine and ultrafine particles (Table 20.13) due to the consistent relationship between particle surface area dose and PMN response (whether particle size is fine or ultrafine) (Tran et al. 1999; Oberdörster et al. 1994). To calculate the critical dose as particle mass per whole lung in humans, the critical dose as particle surface area (m^2 TiO_2/g lung) was divided by the particle specific surface area (m^2 TiO_2/g TiO_2) and multiplied by the human lung mass (assumed to be 1000 g vs. 1 g in rats) (Table 20.13) (Kuempel et al. 2005; NIOSH 2005).

The critical dose estimates as particle surface area were converted to mass dose because the lung dosimetry models are mass-based, as are workplace exposure limits. In addition to the interstitial/sequestration model described here (Section 20.6), the MPPD human lung dosimetry model (CIIT & RIUM 2002) was used for comparision. These models were used to estimate the airborne concentrations of either fine or ultrafine TiO_2 over a 45-year working lifetime that would be associated with an increase in pulmonary inflammation, derived from the rat data (Table 20.13) (Kuempel et al. 2005; NIOSH 2005). The arithmetic mean parameter estimates for K_T and K_{LN} from Tran and Buchanan (2000) were used in the interstitial/sequestration model since those values were based on the larger U.K. miner cohort with more detailed exposure data than the U.S. study. The two lung dosimetry models (MPPD and interstitial/sequestration) provided similar estimates, although the MPPD model predicted higher airborne concentrations by a factor of approximately two, due to prediction of lower lung burdens by the same factor. In other words, the interstitial/sequestration model predicted higher average lung burdens for a given external exposure than did the MPPD model. The MPPD model uses the ICRP (1994) clearance model, which includes three first-order clearance rate coefficients for the alveolar region and has been shown previously to predict lower lung burdens than the interstitial/sequestration model (Kuempel and Tran 2002). Deposition was similar in both models, as the estimated fractional deposition from the MPPD model (CIIT & RIUM 2002) was also used as the deposition fraction in the interstitial/sequestration clearance model.

TABLE 20.12
Sensitivity of Best Group-Fit Model Parameters for Deposition and Clearance among Miners with Lymph Node Data ($n = 57$)

Parameter and Specified Change from Initial Value[a]	Mean Squared Error	Mean Bias (g)	Mean Predicted Lung Dust Burden (g)	Percent Change in Output with 10% Change in Input[b]	Mean Predicted Lymph Node Dust Burden (g)	Percent Change in Output with 10% Change in Input[c]
Default values[d]	95.2	+0.99	14.2	—[e]	1.41	—[e]
F_D +10%	101.0	−0.59	15.6	+9.8	1.55	+9.9
F_D −10%	95.5	+2.3	12.9	−9.2	1.30	−7.8
K_T +10%	94.0	+2.0	13.3	−6.3	1.33	−5.7
K_T −10%	98.6	−0.15	15.2	+7.0	1.50	+6.4
K_I +10%	98.1	+0.03	15.0	+5.6	1.50	+6.4
K_I −10%	93.8	+2.0	13.2	−7.0	1.31	−7.1
K_{LN} +10%	95.0	+1.0	14.0	−1.4	1.54	+9.2
K_{LN} −10%	95.5	+1.0	14.3	+0.7	1.28	−9.2

[a] F_D, fractional deposition; first-order rate coefficients; K_T, alveolar macrophage-mediated clearance of particles to the tracheobronchi; K_I, transfer of particles to the interstitium; K_{LN}, translocation of particles to the hilar lymph nodes.

[b] Output is mean predicted lung burden.

[c] Output is mean predicted lymph node burden.

[d] $F_D = 0.12$; $K_T = 8.8\times10^{-4}\ d^{-1}$; $K_I = 4.5\times10^{-4}\ d^{-1}$; $K_{LN} = 1.0\times10^{-5}\ d^{-1}$.

[e] Not applicable because percent change is relative to the default values.

Source: From Kuempel, E.D., Tran, C.L., Smith, R. J., and Bailer, A. J., *Reg. Toxicol. Pharmacol.*, 34, 88–101, 2001b. With permission.

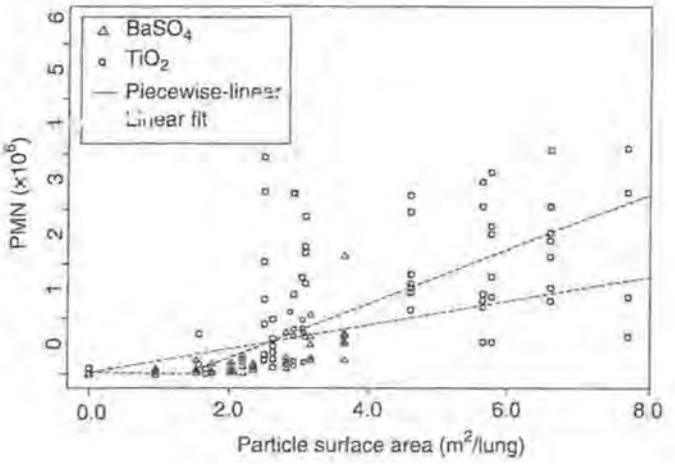

FIGURE 20.12 Piecewise-linear and linear model fits to rat data on pulmonary inflammation (PMN count) and particle surface area dose of titanium dioxide. (Data from Tran, C. L., Cullen, R. T., Buchanan, D., Jones, A. D., Miller, B. G., Searl, A., Davis, J. M. G., and Donaldson, K. Investigation and Prediction of pulmonary responses to dust. Part II. In *Investigations into the Pulmonary Effects of Low Toxicity Dusts*. Parts I and II., Health and Safety Executive, Suffolk, UK, Contract Research Report 216/1999, 1999.)

TABLE 20.13
Airborne Mass Concentrations of Fine and Ultrafine TiO_2 (Over a 45-Year Working Lifetime) and Human-Equivalent Lung Burdens Associated with Pulmonary Inflammation in Rats

	Human-Equivalent Critical Lung Dose: MLE (95% LCL)		Mean Airborne Exposure Concentration: MLE (95% LCL) (mg/m^3)	
Particle size	Particle Surface Area (cm^2/g lung)	Particle Mass (g/lung)	Multiple-Path Particle Deposition (MPPD) Lung Model (CIIT & RIVM 2002) (mg/m^3)	Interstitial Lung Model (Kuempel et al. (2001a, 2001b) and; Tran and Buchanan 2000) (mg/m^3)
Fine (2.1 μm MMAD, 2.2 GSD; 6.68 m^2/g)	139 (130)	2.1 (1.9)	2.0 (1.8)	1.1 (0.9)
Ultrafine (0.8 μm MMAD, 1.8 GSD; 48 m^2/g)	139 (130)	0.29 (0.22)	0.22 (0.17)	0.10 (0.08)

Abbreviations: MMAD, mass median aerodynamic diameter; GSD, geometric standard deviation; MLE, Maximum likelihood estimate; 95% LCL, 95% lower confidence limit.

Source: From Kuempel, E. D., Wheeler, M., Smith, R., and Bailer, A. J., *Nanomaterials: A Risk to Health at Work? First International Symposium on Occupational Health Implications of Nanomaterials*, 12–14 October 2004, Buxton, Derbyshire, UK., Health and Safety Executive, U.K., Buxton, 111, 2005; NIOSH, 2005. NIOSH Current Intelligence Bulletin: Evaluation of Health Hazard and Recommendations for Occupational Exposure to Titanium Dioxide. Unpublished Public Review Draft, November 22, 2005. Cincinnati, OH: U.S. Department of Health and Human Services, Public Health Service Centers for Disease Control and Prevention, National Institute for Occupational Safety and Health, 158. Available at: http://www.cdc.gov/niosh/docs/preprint/tio2/pdfs/TiO_2Draft.pdf.

20.7 DISCUSSION

20.7.1 The Contribution of Dosimetric Modeling to Particle Toxicology

In modeling complex biological processes, it is often possible to describe broad trends using simple regression or other statistical models. However, when it is desired to model the evolution of a process over time, and particularly when the status of the process at any time point influences its subsequent course, it is necessary to develop dynamic models based around differential equations. In either case, the model will be more plausible if based upon an understanding of the underlying biological mechanisms.

A model is a mathematical equation or system of equations that, given quantitative inputs, predicts certain outputs; and, given the same inputs, the output prediction will always be the same. In considering the relevance of model predictions to real-life situations involving populations of animals or of humans, there is an additional need to allow for the variation to be expected in any such population.

The present work has extended our earlier deterministic rat lung dosimetry model by allowing stochastic variation in the parameters, which in turn induces variation in the outputs. Since the input variation is under our control and known, we can investigate the relationships between input and output variation. Such investigations are commonly labeled "sensitivity analysis" when the focus is on the effect of small variations in the inputs, and "uncertainty analysis" when we consider the entire range of variation (Saltelli, Chan, and Scott 2000). In the rat model presented here, we have used Monte Carlo simulation, with plausible assumptions for parameter variation, to generate a pseudo-sample of 1000 instances from an idealized population of rats. By extrapolating the results from this exposure–dose–response model in rats to humans, we have predicted exposure concentrations of poorly soluble particles such as TiO_2 that are not expected to result in lung clearance overload and the onset of inflammation in most workers. We believe that our approach to this problem is novel, by using biomathematical lung models in the risk assessment of poorly soluble particles including nanoparticles.

It is clear that these extensions to the basic process of dynamic modeling introduce a number of new assumptions, and that the plausibility of the results rests in large part on the plausibility of the assumptions, in particular on the implied ranges of variability. At the same time, biomathematical lung models can play an integral role in research on the toxicokinetics of inhaled particles. These models are useful in the design of experimental studies, such as by identifying the research and data needs to validate key parameters and by facilitating the generation and testing hypotheses on biological mechanisms.

The rat lung dosimetry model described here was extrapolated to humans by using human parameter values where available (e.g., the deposition fraction) and by using appropriate allometric scaling methods when human parameter values were not available and needed to be estimated. Data available from literature (Hattis et al. 2001) regarding the variation in some key parameters in humans, such as the deposition fraction and clearance rate, have shown a much wider variation than the observed variation in animal data. This was no surprise as the rats are all from the same strain and the same supply.

A Monte Carlo simulation of the rat biomathematical model extrapolated to humans,predicted that for a working life-time exposure to fine TiO_2 at 4 $mg \cdot m^{-3}$, only 70 percent of the population would avoid overload (Section 20.5.2.2). A concentration level such that 95 percent of the population would avoid overload was found to be 1.3 $mg \cdot m^{-3}$. At this level, the PMN number was not elevated (Figure 20.9). Therefore, 1.3 $mg \cdot m^{-3}$ is an estimate of a working lifetime exposure concentration to fine-sized TiO_2 that is not expected to result in lung disease associated with pulmonary inflammation, based on the rat biomathematical lung model extrapolated to humans.

We have also taken a direct approach at modeling the human exposure-dose relationship for respirable particles. For humans, the overloading of lung clearance of particles as observed in rats has

not been demonstrated exposure-dose relationship for respirable particles, although a study of lung dust burdens in retired coal miners showed that particle clearance rates were reduced or even undetectable in some miners (Freedman and Robinson 1988). This finding is consistent with particle overloading in the lungs of rodents, in which clearance becomes impaired at high lung dust burdens and the impairment continues after exposure ceases. However, the findings are also consistent with a sequestration process, in which particles are transferred (as a first-order process) to the interstitial region of the lungs and retained, with very slow clearance to the hilar lymph nodes, as shown in the lung dosimetry modeling in coal miners. We have constructed various models representing different degrees of overload and found that the model structure that provided the best fit to the coal miner data was a higher-order model with an interstitial or sequestration compartment (Kuempel 2000; Kuempel et al. 2001a). The model representing the rat-based overload kinetics did not improve the model fit to the data, although a lesser degree of overloading could not be ruled out. This model structure was validated in an independent study of U.K. coal miners (Tran and Buchanan 2000). In addition, in that study where individual miners' working lifetime quartz exposure data were available, it was shown that quartz translocated to the hilar lymph nodes at a faster rate than coal dust. The optimized parameter values were consistent with but not identical in the two cohorts.

The human model structure with an interstitial or sequestration compartment is consistent with the observations in retired coal miners (Freedman and Robinson 1988) and with observation of particle retention in the interstitium of human lungs (Nikula et al. 1997). This human model structure is compatible with some of the animal models, which include both sequestration compartments and dose-dependent overloading (Strom, Johnson, and Chan 1989; Stöber et al. 1990a, 1990b; Stöber, 1999; Tran et al. 1999, 2000), although the additional overloading pathway was not needed to fit the coal miner data. A principal difference in this human model compared to the ICRP and NCRP models is that it treats the alveolar and interstitial regions of the lung as separate compartments, which reflects both the biological structure of the lungs and the disposition of particles in these regions.

Further research is needed on whether interspecies differences in particle retention sites within the lungs may influence the sensitivity to a given lung dust burden, and influence the disease response. The findings from this study also suggest that a human lung dosimetry model without an interstitialization or sequestration compartment would not be adequate for predicting the end-of-life lung dust burdens in humans—at least not among those with high dust exposures such as coal miners (Kuempel and Tran 2002). Other data sets, particularly those including individuals with low exposures, are needed for further validation of this model and are ongoing.

Finally, we have also used a more empirical approach, based on a statistical model, to estimate a threshold lung burden of fine and ultrafine TiO_2 at which pulmonary inflammation begins in rats (Section 20.6.3). This estimate of a critical lung dose at which pulmonary inflammation begins is assumed to be equivalent in rats and humans. That is, in the absence of human data, an equivalent particle surface area dose in the lungs in either species is assumed to elicit an equal inflammation response. Next, the human lung dosimetry models were used to estimate the working lifetime exposure concentration that would lead to an equivalent critical lung burden (Table 20.13). These results show that, as expected, the mass airborne concentrations associated with a given particle surface area dose in the lungs is lower for ultrafine TiO_2 than for fine TiO_2. This is due to the dose-response relationship between particle surface area dose and pulmonary inflammation, and to the higher surface area per unit mass of ultrafine TiO_2 compared to fine TiO_2 . Despite the different biomathematical and statistical models used to fit the rat data, the risk estimates are similar. The lower bound estimates for fine-sized TiO_2 (95% LCL of 0.9 or 1.8 mg/m^3) (Table 20.13), based on the statistical modelling of the rat doseresponse data and the human biomathematical exposure-dose model, are similar to the 95% LCL (1.3 mg/m^3) estimated earlier using the rat biornathematical exposuredose-response model extrapolated to humans (Section 20.5.2.2). This consistency across models, rat and human, with species-appropriate parameter values, provides some validation of the models for use in risk assessment. These estimates are provided for illustration only of the use of biornathematical lung models in risk assessment, and it is beyond the scope

of this chapter to discuss the many issues that are considered in a full risk assessment. For example, it should be noted that none of these exposure estimates include adjustment by "safety" or "uncertainty" factors, which are often used in risk assessment to account for uncertainty in factors including extrapolation from animals to humans, interindividual variability, and subchronic to chronic effects (Jarabek et al. 2005). The use of biologically-based models may eliminate the need for some of these uncertainty factors, for example, by accounting for the kinetic differences that influence the exposure-dose relationship in animals and humans.

20.7.2 Issues in the Dosimetry of Nanoparticles

An important area for future lung dosimetry model development is extension of current validated models to include the translocation of particles. Short-term rodent studies have shown that nanoparticles are retained in the lungs to a greater extent than larger respirable particles (Ferin, Oberdörster, and Penney 1992; Oberdörster, Ferin, and Lehnert 1994), which may be due to less effective phagocytosis by AMs (Renwick, Donaldson, and Clouter 2001; Renwick et al. 2004) and increased entry of the nanoparticles into the intersititialization. Nanoparticles may also enter the blood circulation and translocate to other organs, although the rate of translocation may depend on the chemical composition of the particles (Kreyling et al. 2002; Oberdörster et al. 2002; Geiser et al. 2005). In contrast, in a study of the long-term (up to 6 months) clearance of iridium nanoparticles, the lung retention was found to be similar to that reported previously for other poorly soluble, micrometer-sized particles (Semmler et al. 2004). Comparison of observed vs. model-predicted lung burdens in rats show that some rat lung dosimetry models (Tran et al. 2000; Tran, Graham, and Buchanan 2001; Tran et al. 2002; CIIT and RIVM 2002) predict reasonably well the retained mass lung burdens in rats exposed by chronic inhalation to ultrafine or fine poorly soluble particles (Kuempel et al. 2006). More study is needed on the role of particle characteristics, such as chemical composition, surface charge, and size, on the translocation of inhaled particles. In humans, the translocation rate of quartz particles to the lung-associated lymph nodes was estimated to be greater than that for coal particles (Tran and Buchanan 2000), a finding consistent with pathology data (Seaton and Cherrie 1998).

Because of the limited and somewhat contradictory data, it is not certain to what extent the current mass-based lung dosimetry models may predict the clearance and translocation of respirable particles of various size and composition. These models describe the mass transfer of *all* particles that deposit in a given region of the respiratory tract. Since lung deposition models describe particle size-specific deposition in each major region of the respiratory tract, these models inherently allow for particle size-specific clearance to the extent that the particles are subject to clearance by the biological mechanisms of a given respiratory tract region. However, if the efficiency of the particle clearance mechanisms within a lung region vary with particle size, as in the lung airways (Kreyling and Scheuch 2000), then current clearance/retention models may need to be revised to account for this difference. In addition, current models may need to be extended to include pathways for the direct translocation of nanoparticles to the blood circulation and to other organs beyond the lungs. Some models include pathways for dissolution of soluble particles (e.g., Yu, Yoon, and Chen 1991; ICRP 1994). In addition, current models may need to be extended to include other routes of exposure besides inhalation, including dermal, ingestion, or even translocation of nanoparticles along the olfactory nerve into the brain, as reported by Oberdörster et al. (2004) in rats. Before lung dosimetry models in rats or humans are extended to describe the disposition of inhaled nanoparticles, the model structure needs to be validated using existing data of fine and ultrafine particles. The rat and human models described in this chapter are biologically based, validated models of the long-term clearance and retention in the alveolar region of the lungs. Given the many existing lung dosimetry models for particle deposition and clearance, for practical purpose, it would be worthwhile to harmonize these various model structures to the extent possible, including integrating validated models in one format for use and additional development.

ACKNOWLEDGMENT

The authors would like to acknowledge Matt Wheeler, NIOSH, for fitting the piecewise linear model to the rat data and for preparing Figure 20.12.

REFERENCES

ACGIH, TLVs® and BEIs® Based on the Documentation of the Threshold Limit Values for Chemical Substances and Physical Agents & Biological Exposure Indices. American Conference of Governmental Industrial Hygienists, Cincinnati, Ohio, U.S.A., Appendix C, 74–77, 2005.

Adamson, I. Y. and Hedgecock, C., Patterns of particle deposition and retention after instillation to mouse lung during acute injury and fibrotic repair, *Exp. Lung Res.*, 21 (5), 695–709, Sep–Oct. 1995.

Bailey, M. R., Fry, F. A., and James, A. C., Long-term retention of particles in the human respiratory tract, *J. Aerosol. Sci.*, 16(4), 295–305, 1985.

Bermudez, E., Mangum, J. B., Asgharian, B., Wong, B. A., Reverdy, E. E., Janszen, D. B., Hext, P. M., Warheit, D. B., and Everitt, J. I., Long-term pulmonary responses of three laboratory rodent species to subchronic inhalation of pigmentary titanium dioxide particles, *Toxicol. Sci.*, 70 (1), 86–97, 2002.

Bermudez, E., Mangum, J. B., Wong, B. A., Asgharian, B., Hext, P. M., Warheit, D. B., and Everitt, J. I., Pulmonary responses of mice, rats, and hamsters to subchronic inhalation of ultrafine titanium dioxide particles, *Toxicol. Sci.*, 77, 347–357, 2004.

Churg, A. M. and Stevens, B., Association of lung cancer and airway particle concentration, *Environ. Res.*, 45(1), 58–63, 1988.

Churg, A., Brauer, M., del Carmen Avila-Casado, M., Fortoul, T. I., and Wright, J. L., Chronic exposure to high levels of particulate air pollution and small airway remodeling, *Environ. Health Perspect.*, 111 (5), 714–718, 2003.

CIIT and RIVM, Multiple-path particle deposition: a model for human and rat airway particle dosimetry, v.1.0. Research Triangle Park, NC: CIIT Centers for Health Research (CIIT) and The Netherlands: National Institute for Public Health and the Environment (RIVM), 2002.

Crapo, J. D., Young, S. L., Fram, E. K., Pinkerton, K. E., Barry, B. E., and Crapo, R. O., Morphometric characteristics of cells in the alveolar region of mammalian lungs, *Am. Rev. Respir. Dis.*, 128, S42–S46, 1983.

Crapo, J. D., Chang, Y. L., Miller, F. J., and Mercer, R. R., Aspects of respiratory tract structure and function important for dosimetry modeling: Interspecies comparisons, In *Principles of Route-to-Route Extrapolation for Risk Assessment*, Gerrity, J. R. and Henry, C. J., eds., Elsevier, New York, 15–32, 1990.

Dethloff, L. A. and Lehnert, B. E., Pulmonary interstitial macrophages: isolation and flow cytometric comparisons with alveolar macrophages and blood monocytes, *J. Leukocyte Biol.*, 43, 80–90, 1988.

Donaldson, K. and Tran, C. L., Inflammation caused by particles and fibers, *Inhal Toxicol*, 14 (1), 5–27, 2002.

Elder, A, Gelein, R., Finkelstein, J. N., Driscoll, K. E, Harkema, J., Oberdörster, G., Effects of subchronically inhaled carbon black in three species. I. retention kinetics, lung inflammation, and histopathology. *Toxicol Sci.*, [Epub ahead of print], 2005.

Ferin, J., Oberdörster, G., and Penney, D. P., Pulmonary retention of ultrafine and fine particles in rats, *Am. J. Respir. Cell Mol. Biol.*, 6, 535–542, 1992.

Freedman, A. P. and Robinson, S. E., Noninvasive magnetopneumographic studies of lung dust retention and clearance in coal miners, In *Respirable Dust in the Mineral Industries: Health Effects, Characterization and Control*, Frantz, R. L. and Ramani, R. V., eds., The Pennsylvania State University, University Park, PA, 181–186, 1988.

Geiser, M., Rothen-Rutishauser, B., Kapp, N., Schurch, S., Kreyling, W., Schulz, H., Semmler, M., Im Hof, V., Heyder J, J., and Gehr, P., Ultra-fine particles cross cellular membranes by nonphagocytic mechanisms in lungs and in cultured cells, *Environ. Health Perspect.*, 113 (11), 1555–1560, 2005.

Hattis, D., Goble, R., Russ, A., Banati, P., and Chu, M., Human interindividual variability in susceptibility to airborne particles, *Risk Anal.*, 21(4), 585–599, 2001.

ICRP, Human respiratory tract model for radiological protection. A report of a task group of the International Commission on Radiological Protection, Elsevier Science Inc., Tarrytown, New York, ICRP Publication No. 66, 1994.

Ings, R.M., Interspecies scaling and comparisons in drug development and toxicokinetics, *Xenobiotica*, 20 (11), 1201–1231, 1990.

Jarabek, A. M., Asgharian, B., and Miller, F. J., Dosimetric adjustments for interspecies extrapolation of inhaled poorly soluble particles (PSP), *Inhal. Toxicol.*, 17 (7–8), 317–334, 2005.

Jones, A. D., Vincent, J. H., McMillan, C. H., Johnston, A. M., Addison, J., McIntosh, C., Whittington, M. S., Cowie, H., Parker, I., Donaldson, K., and Bolton, R. E., Animal studies to investigate the deposition and clearance of inhaled mineral dusts, Final report on CEC Contract 7248/33/026. Institute of Occupational Medicine, Edinburgh, (IOM Report TM/88/05), 1988.

Koblinger, L. and Hofmann, W., Analysis of human lung morphometric data for stochastic aerosol deposition calculations, *Phys. Med. Biol.*, 30 (6), 541–556, 1985.

Koblinger, L. and Hofmann, W., Monte Carlo modeling of aerosol deposition in human lungs. Part I: simulation of particle transport in stochastic lung structure, *J. Aerosol Sci.*, 21, 661–674, 1990.

Kreyling, W. G. and Scheuch, G., Clearance of particles deposited in the lungs, In *Particle-Lung Interactions*, Gehr, P. and Heyder, J., eds., Marcel Dekker, Inc., New York, 323–376, 2000.

Kreyling, W. G., Semmler, M., Erbe, F., Mayer, P., Takenaka, S., Schulz, H., Oberdörster, G., and Ziesenis, A., Translocation of ultrafine insoluble iridium particles from lung epithelium to extrapulmonary organs is size dependent but very low. *J. Toxicol. Env. Health Pt A*, 65 (20), 1513–1530, 2002.

Kuempel, E. D., Comparison of human and rodent lung dosimetry models for particle retention, *Drug Chem. Toxicol.*, 23 (1), 203–222, 2000.

Kuempel, E. D. and Tran, C. L., Comparison of human lung dosimetry models: implications for risk assessment, *Ann. Occup. Hyg.*, 46 (suppl. 1), 337–341, 2002.

Kuempel, E. D., O'Flaherty, E. J., Stayner, L. T., Attfield, M. D., Green, F. H. Y., and Vallyathan, V., Relationships between lung dust burden, pathology, and lifetime exposure in an autopsy study of U.S. coal miners, *Ann. Occup. Hyg.*, 41 (suppl. 1), 384–389, 1997.

Kuempel, E. D., O'Flaherty, E. J., Stayner, L. T., Smith, R. J., Green, F. H. Y., and Vallyathan, V., A biomathematical model of particle clearance and retention in the lungs of coal miners. Part I. Model development, *Reg. Toxicol. Pharmacol.*, 34, 69–87, 2001a.

Kuempel, E. D., Tran, C. L., Smith, R. J., and Bailer, A. J., A biomathematical model of particle clearance and retention in the lungs of coal miners. Part II. Evaluation of variability and uncertainty, *Reg. Toxicol. Pharmacol.*, 34, 88–101, 2001b.

Kuempel, E. D., Wheeler, M., Smith, R., and Bailer, A. J., Quantitative risk assessment in workers using rodent dose–response data of fine and ultrafine titanium dioxide. [Abstract], In *Nanomaterials: A Risk to Health at Work? First International Symposium on Occupational Health Implications of Nanomaterials*, 12–14 October 2004, Buxton, Derbyshire, UK., Health and Safety Executive, U.K., Buxton, 111, 2005.

Kuempel, E. D., Tran, C. L., Bailer, A. J., Castranova, V., Lung dosimetry models in rats and humans: use and evaluation for risk assessment of nanoparticles, *Inhal. Toxicol.*, 2006 *in press*.

Martonen, T. B., Rosati, J. A., and Isaacs, K. K., Modeling deposition of inhaled particles, In *Aerosols Handbook: Measurement, Dosimetry, and Health Effects*, Ruzer, L. S. and Harley, N. H., eds., CRC Press, Boca Raton, Florida, 113–155, 2005.

Mauderly, J. L., Lung overload: the dilemma and opportunities for resolution, In *Particle Overload in the Rat Lung and Lung Cancer, Implications for Human Risk Assessment*, Proceedings of a conference held at the Massachusetts Institute of Technology, Mauderly, J. L., and McCunney, R. J., eds., March 29–30, 1995, Taylor and Francis, Washington, DC, 1–28, 1996.

McClellan, R. O., Particle interactions with the respiratory tract, In *Particle-Lung Interactions*, Gehr, P. and Heyder, J., eds., Marcel Dekker, Inc., New York, 1–63, 2000. Chapter 1.

Ménache, M. G., Miller, F. J., and Raabe, O. G., Particle inhalability curves for humans and small laboratory animals, *Ann. Occup. Hyg.*, 39, 317–328, 1995.

Miller, F. J., Dosimetry of particles in laboratory animals and humans, In *Toxicology of the Lung*, Gardner, D. E., Crapo, J. D., and McClellan, R. O., eds. 3rd ed., Taylor and Francis, Philadelphia, PA, 513–556, 1999. Chapter 18.

Morrow, P. E., Possible mechanisms to explain dust overloading of the lungs, *Fund. Appl. Toxicol.*, 10, 369–384, 1988.

Mortensen, J. D. et al., Age related morphometric analysis of human lung casts, *Extrapolation of Dosimetric Relationships for Inhaled Particles and Gases*, Academic Press, San Diego, CA, 59–68, 1988.

Muhle, H., Creutzenberg, O., Bellmann, B., Heinrich, U., Ketkar, M., and Mermelstein, R., Dust overloading of lungs: investigations of various materials, species differences, and ireversibility of effects, *J. Aerosol Med.*, 3 (suppl. 3), S111–S128 1990.

NCRP, Deposition, retention, and dosimetry of inhaled radioactive substances, *National Council on Radiation Protection and Measurements*, Bethesda, MD. Report No. 125, 253, 1997.

Nikula, K. J., Avila, K. J., Griffith, W. C., and Mauderly, J. L., Lung tissue responses and sites of particle retention differ between rats and cynomolgus monkeys exposed chronically to diesel exhaust and coal dust, *Fundam. Appl. Toxicol.*, 37, 37–53, 1997.

NIOSH, 2005. NIOSH Current Intelligence Bulletin: Evaluation of Health Hazard and Recommendations for Occupational Exposure to Titanium Dioxide. Unpublished Public Review Draft, November 22, 2005. Cincinnati, OH: U.S. Department of Health and Human Services, Public Health Service Centers for Disease Control and Prevention, National Institute for Occupational Safety and Health, 158, Available at: http://www.cdc.gov/niosh/docs/preprint/tio$_2$/pdfs/TIO$_2$Draft.pdf.

Oberdörster, G., Ferin, J., and Lehnert, B. E., Correlation between particle size in vivo particle persistence, and lung injury, *Environ. Health Perspect.*, 102 (suppl. 5), 173–179, 1994.

Oberdörster, G., Sharp, Z., Atudorei, V., Elder, A., Gelein, R., Lunts, A., Kreyling, W., and Cox, C., Extrapulmonary translocation of ultrafine carbon particles following whole-body inhalation exposure of rats, *J. Toxicol. Environ. Health Pt. A*, 65 (20), 1531–1543, 2002.

Oberdörster, G., Sharp, Z., Atudorei, V., Elder, A., Gelein, R., Kreyling, W., and Cox, C., Translocation of inhaled ultrafine particles to the brain, *Inhal. Toxicol.*, 16 (6–7), 437–445, 2004.

O'Flaherty, E. J., Interspecies conversion of kinetically equivalent doses, *Risk Analysis*, 9 (4), 587–598, 1989.

Parent, R. A., *Treatise on Pulmonary Toxicology: Comparative Biology of the Normal Lung*, Vol. 1, CRC Press, Boca Raton, 1992.

Raabe, O.G., Yeh, H.C., Newton, G.J., Phalen, R.F., and Velasquez, D.J., Deposition of inhaled monodisperse aerosols in small rodents. In Inhaled Particles IV. Proceedings of an' international symposium organised by the British Occupational Hygiene Society, Edinburgh, 22–26, September 1975. Vol. 1. Oxford: Pergamon Press: 3–21, 1977.

Raabe, O.G., Al-Bayati, M.A., Teague, S.V., Rasolt, A., Regional deposition of monodisperse coarse and fine aerosol particles in small laboratory animals, In *Inhaled Particles VI. Proceedings of an international symposium and workshop on Lung Dosimetry organized by the British Occupational Hygiene Society in co-operation with the Commission of the European Communities*, Cambridge, 2–6, September 1985. Pergamon Press, Oxford, 53–64. (Ann. Occup. Hyg.; 32 (suppl.1)), 1988.

Renwick, L. C., Donaldson, K., and Clouter, A., Impairment of alveolar macrophage phagocytosis by ultrafine particles, *Toxicol. Appl. Pharmacol.*, 172 (2), 119–127, 2001.

Renwick, L. C., Brown, D., Clouter, A., and Donaldson, K., Increased inflammation and altered macrophage chemotactic responses caused by two ultrafine particles, *Occup. Environ. Med.*, 61, 442–447, 2004.

Reynolds, H. Y., Lung inflammation and fibrosis: an alveolar macrophage-centered perspective from the 1970s to 1980s, *Am. J. Respir. Crit. Care Med.*, 171 (2), 98–102, 2005.

Saltelli, A., Chan, K., and Scott, M., eds., Sensitivity Analysis, John Wiley & Sons publishers, Probability and Statistics series, 2000.

Seaton, A. and Cherrie, J. W., Quartz exposures and severe silicosis: a role for the hilar nodes, *Occup. Environ Med.*, 55 (6), 383–386, 1998.

Semmler, M., Seitz, J., Erbe, F., Mayer, P., Heyder, J., Oberdörster, G., and Kreyling, W. G., Long-term clearance kinetics of inhaled ultrafine insoluble iridium particles from the rat lung, including transient translocation into secondary organs, *Inhal. Toxicol.*, 16 (6–7), 453–459, 2004.

Snipes, M. B., Long-term retention and clearance of particles inhaled by mammalian species, *CRC Crit. Rev. Toxicol.*, 20 (3), 175–211, 1989.

Stahlhofen, W., Scheuch, G., and Bailey, M. R., Investigations of retention of inhaled particles in the human bronchial tree, *Radiat. Prot. Dosim.*, 60, 311–319, 1995.

Stöber, W., Morrow, P. E., and Hoover, M. D., Compartmental modeling of the long-term retention of insoluble particles deposited in the alveolar region of the lung, *Fund. Appl. Toxicol.*, 13, 823–842, 1989.

Stöber, W., Morrow, P. E., and Morawietz, G., Alveolar retention and clearance of insoluble particles in rats simulated by a new physiology-oriented compartmental kinetics model, *Fund Appl. Toxicol.*, 15, 329–349, 1990a.

Stöber, W., Morrow, P. E., Morawietz, G., Koch, W., and Hoover, M., Developments in modeling alveolar retention of inhaled insoluble particles in rats, *J. Aerosol Med.*, 3 (suppl. 1), 129–154, 1990b.

Stöber, W., Morrow, P.E., Koch, W., Morawietz, G. Alveolar clearance and retention of inhaled soluble particles in rats simulated by a model inferring macrophage particle load distributions. *J. Aerosol Sci.* 25, 975–1002, 1994.

Strom, K. A., Johnson, J. T., and Chan, T. L., Retention and clearance of inhaled submicron carbon black particles, *J. Toxicol. Environ. Health*, 26, 183–202, 1989.

Tran, C. L., Buchanan, D., Development of a biomathematical lung model to describe the exposure-dose relationship for inhaled dust among UK coal miners. Institute of Occupational Medicine, Edinburgh, UK, IOM Research Report TM/00/02, 2000.

Tran, C. L., Jones, A. D., and Donaldson, K., Overloading of particles and fibres, *Ann. Occup. Hyg.*, 41(suppl. 1), 237–243, 1997.

Tran, C. L., Cullen, R. T., Buchanan, D., Jones, A. D., Miller, B. G., Searl, A., Davis, J. M. G., and Donaldson, K., Investigation and prediction of pulmonary responses to dust. Part II, In *Investigations Into the Pulmonary Effects of Low Toxicity Dusts. Parts I and II.*, Health and Safety Executive, Suffolk, UK, Contract Research Report 216/1999, 1999.

Tran, C. L., Buchanan, D., Cullen, R. T., Searl, A., Jones, A. D., and Donaldson, K., Inhalation of poorly soluble particles II. Influence of particle surface area on inflammation and clearance, *Inhal. Toxicol.*, 12, 1113–1126, 2000.

Tran, C.L., Graham, M., and Buchanan, D., A biomathematical model for rodent and human lungs describing exposure, dose, and response to inhaled silica. Institute of Occupational Medicine, Edinburgh, U.K., IOM Research Report TM/01/04, 35, 2001.

Tran, C. L., Kuempel, E. D., and Castranova, V., A model of exposure, dose and response to inhaled silica, *Ann. Occup. Hyg.*, 46 (suppl. 1), 14–17, 2002.

Tran, C. L., Miller, B. G., and Jones, A. D., Risk assessment of inhaled particles using a physiologically based mechanistic model. Institute of Occupational Medicine Research Report 141, prepared for the Health and Safety Executive, 47, 2003.

Vallyathan, V., Brower, P. S., Green, F. H. Y., and Attfield, M. D., Radiographic and pathologic correlation of coal workers' pneumoconiosis, *Am. J. Respir. Crit. Care. Med.*, 154, 741–748, 1996.

van Oud Alblas, A. B. and van Furth, R., Origin, kinetics, and characterization of pulmonary macrophages in the normal steady state, *J. Exp. Med.*, 136, 186–192, 1986.

Vincent, J. H., Jones, A. D., Johnston, A. R., Bolton, R. E., and Cowie, H., Accumulation of inhaled mineral dust in the lung and associated lymph nodes: implications to exposure and dose in occupational lung disease, *Ann. Occup. Hyg.*, 31, 375–393, 1987.

Warheit, D. B., Overby, L. H., Beroge, G., and Brody, A. R., Pulmonary macrophages are attracted to inhaled particles through complement activation, *Exp. Lung Res.*, 14, 51–66, 1988.

Yeh, H. C. and Schum, G. M., Models of human lung airways and their application to inhaled particle deposition, *Bull. Math. Biol.*, 42, 461–480, 1980.

Yu, R. C. and Rappaport, S. M., A lung retention model based on Michaelis-Menten-like kinetics, *Environ. Health Perspect.*, 105 (5), 496–503, 1997.

Yu, C. P., Morrow, P. E., Chan, T. L., and Yoon, K. J., A non-linear model of alveolar clearance of insoluble particles from the lung, *Inhal Toxicol*, 1, 97–107, 1988.

Yu, C. P., Yoon, K. J., and Chen, Y. K., Retention modeling of diesel exhaust particles in rats and humans, *J. Aerosol Med.*, 4 (2), 79–115, 1991.

Yu, C. P., Zhang, L., Oberdörster, G., Mast, R. W., Glass, L. R., and Utell, M. J., Clearance of refractory ceramic fibres (RCF) from the rat lung: development of a model. *Environ. Res.* 65, 243–253, 1994.

Zhang, Z. and Martonen, T. B., Deposition of ultrafine aerosols in human tracheobronchial airways, *Inhal Toxicol.*, 9 (2), 99–110, 1997.

CRC Press
Taylor & Francis Group
6000 Broken Sound Parkway NW, Suite 300
Boca Raton, FL 33487-2742

Printed in the United States of America on acid-free paper
10 9 8 7 6 5 4 3 2 1

International Standard Book Number-10: 0-8493-5092-1 (Hardcover)
International Standard Book Number-13: 978-0-8493-5092-4 (Hardcover)

Library of Congress Cataloging-in-Publication Data

Particle toxicology / editors, Ken Donaldson and Paul Borm.
p. ; cm.
Includes bibliographical references and index.
ISBN-13: 978-0-8493-5092-4 (hardcover : alk. paper)
ISBN-10: 0-8493-5092-1 (hardcover : alk. paper)
1. Pulmonary toxicology. 2. Particles--Toxicology. I. Donaldson, Kenneth, DSc. II. Borm, Paul.
[DNLM: 1. Air Pollutants--toxicity. 2. Inflammation. 3. Mineral Fibers--toxicity. 4. Oxidative Stress. WA 754 P2732 2007]

RC720.P373 2007
616.2'00471--dc22 2006037017

Visit the Taylor & Francis Web site at
http://www.taylorandfrancis.com

and the CRC Press Web site at
http://www.crcpress.com

Particle Toxicology

Edited by
Ken Donaldson
Paul Borm

CRC Press
Taylor & Francis Group
Boca Raton London New York

CRC Press is an imprint of the
Taylor & Francis Group, an informa business